Final Report

BRIDGING THE PSI KNOWLEDGE GAPS: A MULTISCALE APPROACH

Principal Investigator: Dennis G. Whyte
Postal Address: MIT Plasma Science and Fusion Center, NW17-119
175 Albany Street
Cambridge, MA 02139

Telephone Number: 617-253-1748
E-mail: whyte@psfc.mit.edu

DOE/Office of Science Program Office: Office of Fusion Energy Sciences

DOE/Office of Science Program Office Contact: Dr. Peter Pappano

DOE/Office of Science Grant: DE-SC00-02060

Table of Contents

Executive Summary

The Plasma Surface Interactions (PSI) Science Center formed by the grant undertook a multidisciplinary set of studies on the complex interface between the plasma and solid states of matter. The strategy of the center was to combine and integrate the experimental, diagnostic and modeling toolkits from multiple institutions towards specific PSI problems. In this way the Center could tackle integrated science issues which were not addressable by single institutions, as well as evolve the underlying science of the PSI in a more general way than just for fusion applications. The overall strategy proved very successful. The research result and highlights of the MIT portion of the Center are primarily described.

A particular highlight is the study of tungsten nano-tendril growth in the presence of helium plasmas. The Center research provided valuable new insights to the mechanisms controlling the nano-tendrils by developing coupled modeling and in situ diagnostic methods which could be directly compared. For example, the role of helium accumulation in tungsten distortion in the surface was followed with unique in situ helium concentration diagnostics developed. These depth-profiled, time-resolved helium concentration measurements continue to challenge the numerical models of nano-tendrils. The Center team also combined its expertise on tungsten nano-tendrils to demonstrate for the first time the growth of the tendrils in a fusion environment on the Alcator C-Mod fusion experiment, thus having significant impact on the broader fusion research effort. A new form of isolated nano-tendril “columns” were identified which are now being used to understand the underlying mechanisms controlling the tendril growth.

The Center also advanced PSI science on a broader front with a particular emphasis on developing a wide range of in situ PSI diagnostic tools at the DIONISOS facility at MIT. For example the strong suppression of sputtering by the certain combination of light-species plasmas and metals was experimentally studied with independent measurement methods across the Center. This surprising result challenges the universal use of the binary-collision approximation in sputtering predictions and continues to be the subject of study. In order to address this issue MIT developed a new in situ erosion measurement technique based on ion beam analysis which can be used at elevated material temperatures. This exciting new technique is now being used to study material erosion in high performance plasma thrusters for space exploration and is being adopted to fusion experimental devices. This is an indicator of the positive synergies that arise from such a Center, with the research having impact beyond the initial area of study.

The Center also served successfully as an organizing force for communication to the science community. The MIT members of the Center provided many high-profile overview presentations at prestigious international conferences and national workshops. The research resulted in three student theses and 24 peer-reviewed publications. PSI research continues to be identified as a critical area for fusion energy.

1. Introduction

It has long been appreciated that plasma-surface interactions (PSI) are one of the most critical issues in magnetic confinement fusion research. The demands on plasma-facing materials in a steady-state fusion device will be extreme. The operational success of future long-pulse burning plasma devices will hinge on PSI issues. These issues are related to the large-scale net modification of surfaces, which will begin to limit the operational viability and availability of the device for physics operations. Some of the most critical PSI issues are 1) the net erosion of plasma-facing surfaces, 2) net tritium fuel retention in surfaces, 3) H isotope and material mixing in the wall, and 4) the minimization of core plasma impurities. While it is widely accepted that the plasma-surface interface sets a critical boundary condition for the fusion plasma, predictive capabilities for PSI remain highly inadequate.

The purpose of the Center research was to focus on improving PSI *science* in order to reduce the knowledge gaps. The Center was multi-institutional with participants also from UCSD, U. Tennessee-Knoxville and Sandia. The Center stresses a multi-pronged approach to PSI Science with each institution bringing a particular toolkit: high power plasma exposure at UCSD, multiscale numerical modeling at UT-K and surface science measurements at Sandia. The development of advanced in situ diagnostics for PSI studies was the particular focus of the efforts at MIT, and this research will be the primary emphasis of this report.

The organization of the report is as follows. In Section 2 the research approach and capabilities of the Center, and the research team gathered at MIT, are described. In Section 3 the PSI Science Center research results are described. In Section 4 community presentations made by the MIT Center team are documented and described. Section 5 documents the publications and theses from the research grant and also serves as the bibliography for the report.

2. Research Approach & Capabilities

2.1. Multiscale Approach to PSI Science

While the need for substantial advances in PSI is obvious, it is necessary to ask in which ways the present "approach" of PSI research is inadequate. Certainly there have been advances but in the continuing judgment of the overall fusion research community, such as recent reports from FESAC, this field has relatively higher scientific and technological hurdles to overcome. To be fair, this is largely imposed by the fact that compared to extrapolations in the other major research fields in fusion (transport, MHD, waves, etc.), the parameters that drive PSI issues, such as energy and fuel throughput, face the largest single step up from present devices to burning plasmas [Whyte_FED12]. In some PSI areas there are fundamental new challenges, such as significant radiation

damage from 14 MeV neutrons. The empirical and phenomenological approach on confinement devices is largely driven by lack of direct diagnosis of surfaces; given the limited physical access to wall materials, PSI results are typically from campaign integrated changes, a sort of "archeological" approach, while the core plasma response is routinely measured. This approach has been successful in overcoming issues towards achieving high performance core plasmas, but it is clearly inadequate in and of itself to extrapolate and predict forward. On the other hand there is a rich history of dedicated laboratory devices, typically ion beam or low temperature plasmas, which have been used to study individual aspects of the PSI such as sputter yields, implantation, atomic rates, etc. Such devices are invaluable since they are designed to garner diagnostic access to the plasma-surface interface and typically have largely externally controlled exposure parameters. However simple direct application of such knowledge, for example sputter yields, gained in "lab" experiments to the confinement environment is not applicable.

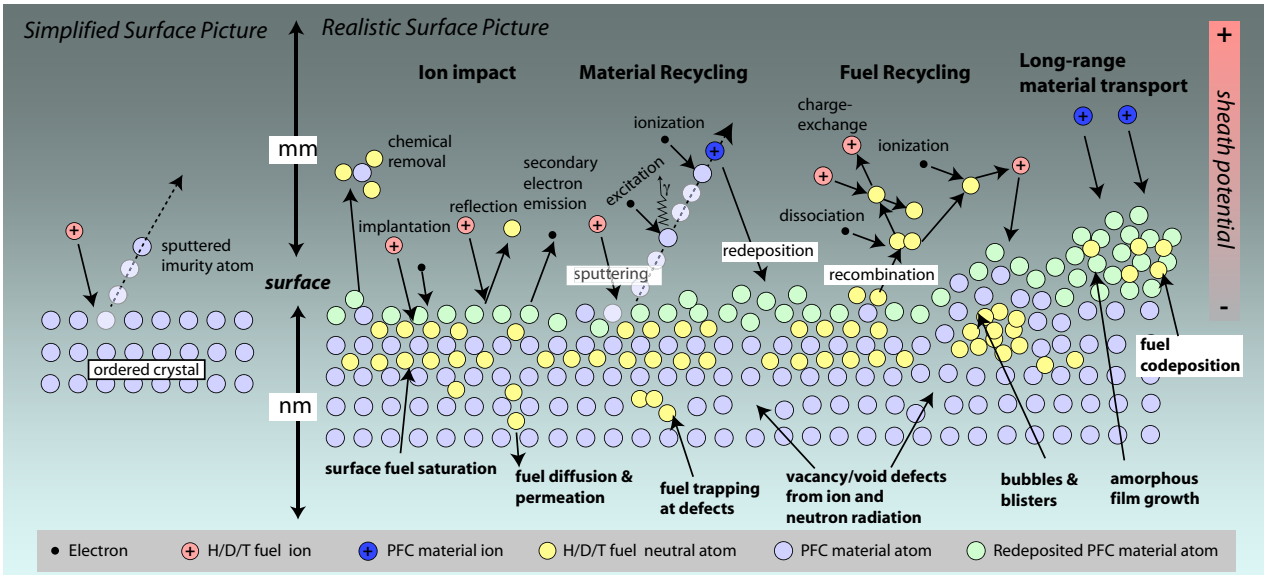

Fig. 1 Schematic illustration of the complex, synergistic and inherently multiscale surface interactions occurring at the material surface in a realistic magnetic fusion plasma environment, in contrast to the simplified picture of ion-induced sputtering from an ordered material.

This can be understood by examining the complexity of plasma-surface interactions in magnetic fusion, shown graphically in Fig. 1. Despite the vastly different physical scales for the surface (~ nm) and plasma processes (~ mm) the plasma and material surface are strongly coupled to each other, mediated by an electrostatic and magnetic sheath. For example, the high probability (> 90%) of prompt local ionization and redeposition for sputtered material atoms, means that the surface material in contact with the plasma is itself a plasma-deposited surface, not the original ordered material of the PFC. Likewise the recycling of plasma fuel (hydrogenic in the case of fusion) is self-regulated through recycling processes involving the near-surface fuel transport in the material and the ionization sink action of the plasma. Also the intense radiation environment (ions, neutrons, photons) ensures that the material properties are modified and dynamically coupled to the PSI processes. Linear, compartmentalized and un-

connected applications of laboratory-measured processes cannot capture the dynamic, interlinked nature of PSI science.

The PSI Science Center has focused on an innovative multiscale approach to PSI sciences. The organizing principle is to develop synergistic experimental, diagnostic and

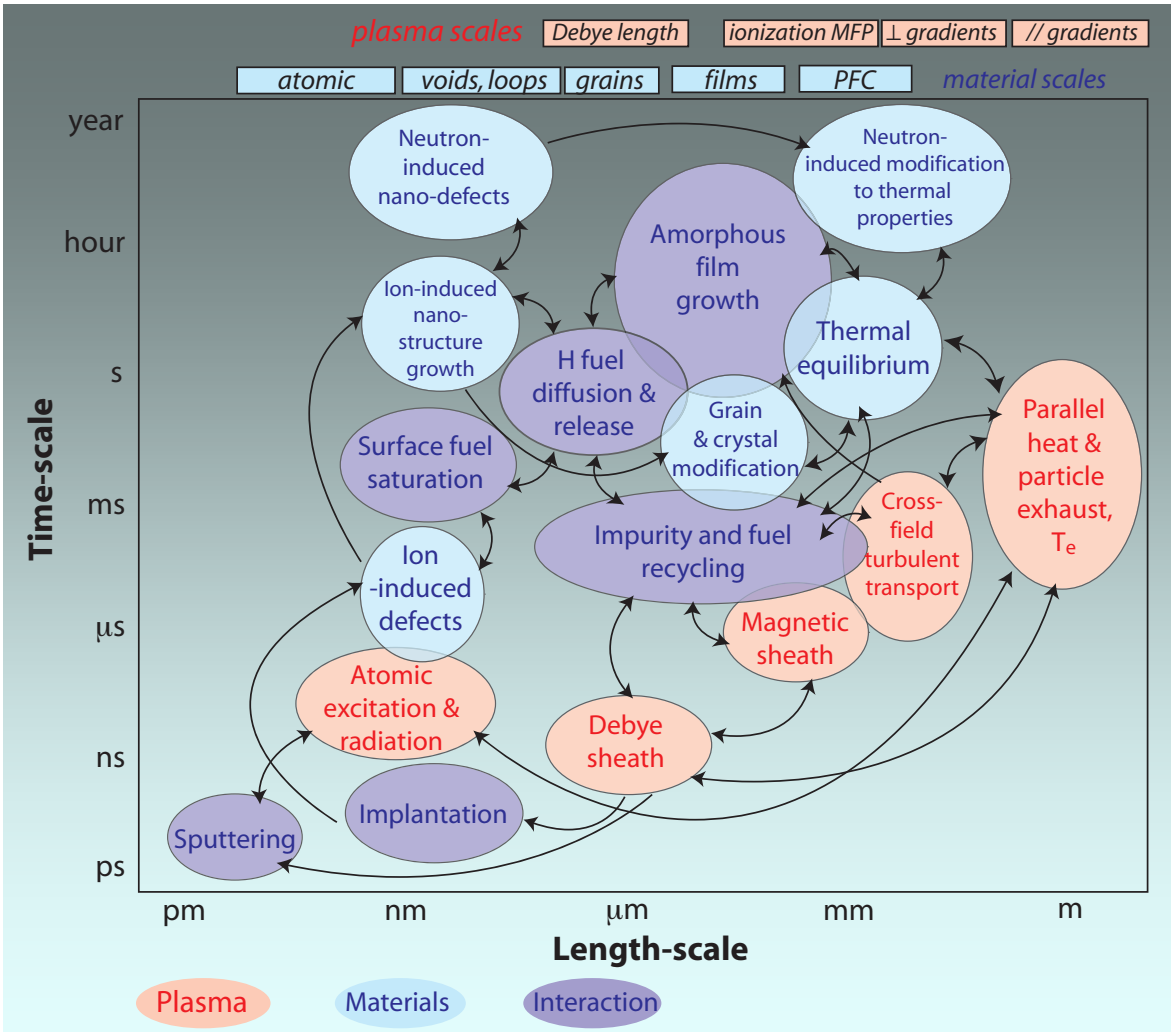

Fig. 2 Graphical representation of multiscale, coupled nature of PSI processes and phenomena in the boundary plasma of magnetic fusion devices.

modeling tools that treat the truly coupled multiscale aspect of the PSI issues. This multiscale view of PSI science is graphically represented in Fig. 2, indicating the extreme spatial and time scales spanned by the coupled plasma-material interactions.

The PSI Center viewpoint was motivated and inspired by the multiscale approach to materials that has been successfully developed over the past decade. Much like PSI science, materials research was previously advanced using empirical and phenomenological methods, the so-called "cook and look" approach. However it was realized that this approach was limited both due to the cost of "cook and look", as well as the lack of predictive capability. The advent of modern computing, and several diagnostic

advances, made it possible to transform materials research to one that was science-based, and which tackled the fundamental multiscale nature of understanding materials from the atomistic to the macroscopic level. Beyond the obvious PSI connection to materials, these observations resonate very closely with the goals of bridging the PSI knowledge gaps shown in Fig. 2. Our assessment is that that the time is right to develop the same science-based approach, and that the necessary tools are available.

The Center was well equipped to deal with the multiscale science due to an exciting confluence of world-class, predominately university-based, experimental and modeling capabilities in the US fusion program. The Center adopted a balanced approach to PSI science with roughly equal emphases on plasma/ion exposure of materials (UCSD) material and plasma diagnostics (MIT), and numerical modeling of plasmas and materials UT-K). The Center efficiently accomplished this ambitious research effort by leveraging existing resources, and by applying strategic upgrades where required. By incorporating all the scale length capabilities, computationally and experimentally, within a single entity the PSI Plasma Center, the Center provided comprehensive coverage of PSI science not available in a single facility, and thereby gained significant scientific synergy from the combination.

The science goal of the PSI Center was to develop predictive capability of PSI issues by probing and understanding at a fundamental level the interactions between the different controlling processes and scale lengths. These issues include erosion of plasma-facing surfaces, control of hydrogenic fuels, power exhaust, plasma impurity contamination and synergistic effects of plasma-induced damage. It is also important to note that while the Center had as its motivation, i.e. the challenging PSI issues associated with magnetic confinement devices, it firmly adhered to a broad *science* approach, as opposed to an applied research approach. For example, it will *not* be within the purview of the Center to test or qualify different plasma-facing materials, nor carry out experiments or modeling towards some specific need of the participating confinement devices. Rather the PSI Center will view all its resources as an integrated research tool towards generally advancing PSI science.

2.2. Research Facilities and Capabilities

The material exposure capabilities of the Center are depicted in Fig. 3. The range of incident ion energies spans essentially the entire range from ~1 eV to ~10 MeV, corresponding to the desired large range of physical scales in the materials ~ nm to mm (proton range in carbon is taken as a example along the top axis). The vertical axis indicates incident flux density (increasing towards the bottom), which can be thought of as an inverse timescale in which to achieve a desired ion fluence or plasma-surface equilibrium. For plasma exposure, increased flux is accompanied by increasing plasma density, and therefore the plasma and surface become more tightly coupled due to the short ionization mean-free paths for sputtered particles (Fig. 1). Also, Fig. 3 shows that inclusion of confinement devices (DIII-D, C-Mod) significantly enhances the Center's ability to access high flux density plasmas with increased plasma-material coupling.

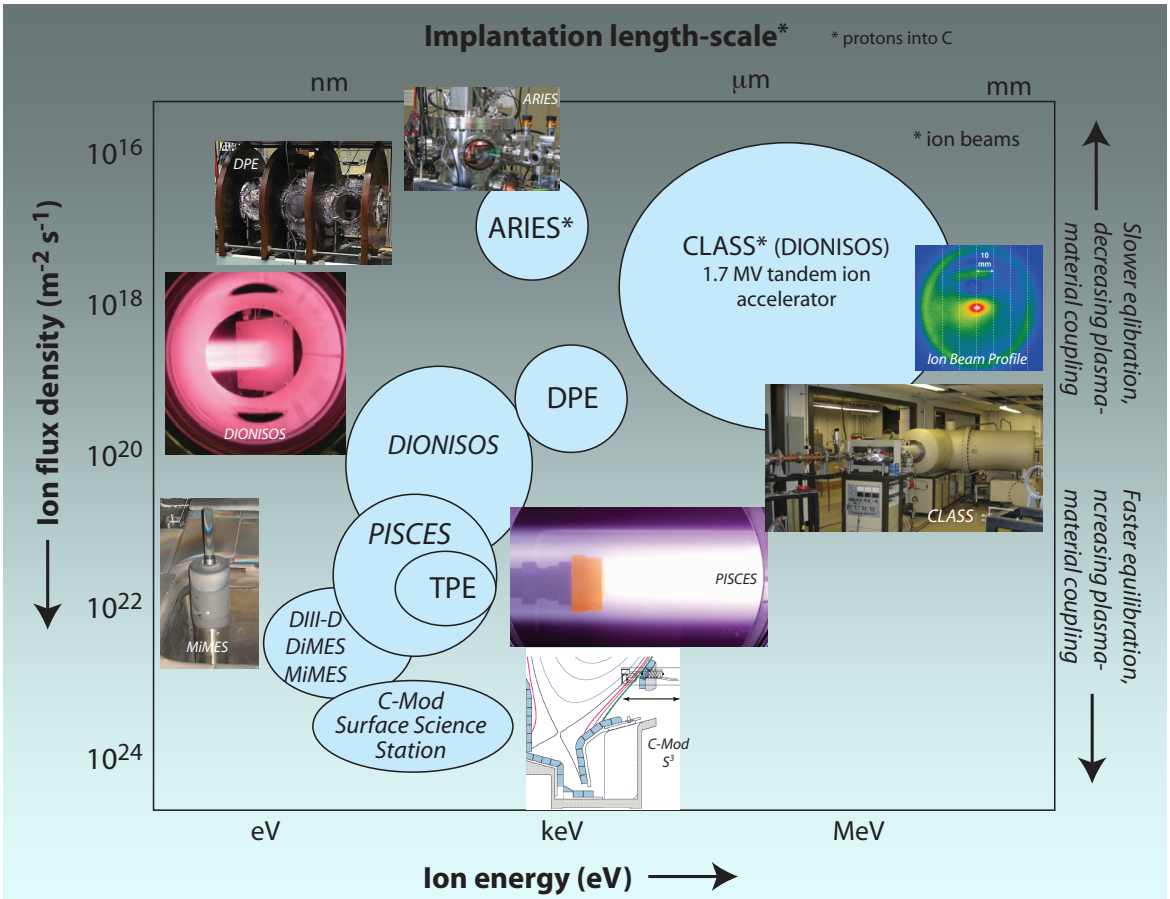

Fig. 3 Multiscale representation of PSI Center capabilities for exposing materials to ions and plasmas. MIT devices (CLASS, DIONISOS and C-Mod) are described in the text.

The PSI diagnostic capabilities of the Center are depicted in Fig. 4. Advancing PSI diagnostic capabilities and coverage was critical to the success of a science-oriented Center. The range of diagnostic coverage is impressive, spanning the required spatial and time scales required for PSI science (Fig. 2), and indicating the potential of combining multiple facilities into a single entity through the Center towards a common science goal. Another strength is that the majority of the MIT diagnostics are in-situ, with particular examples being ion beam analysis (IBA) on DIONISOS.

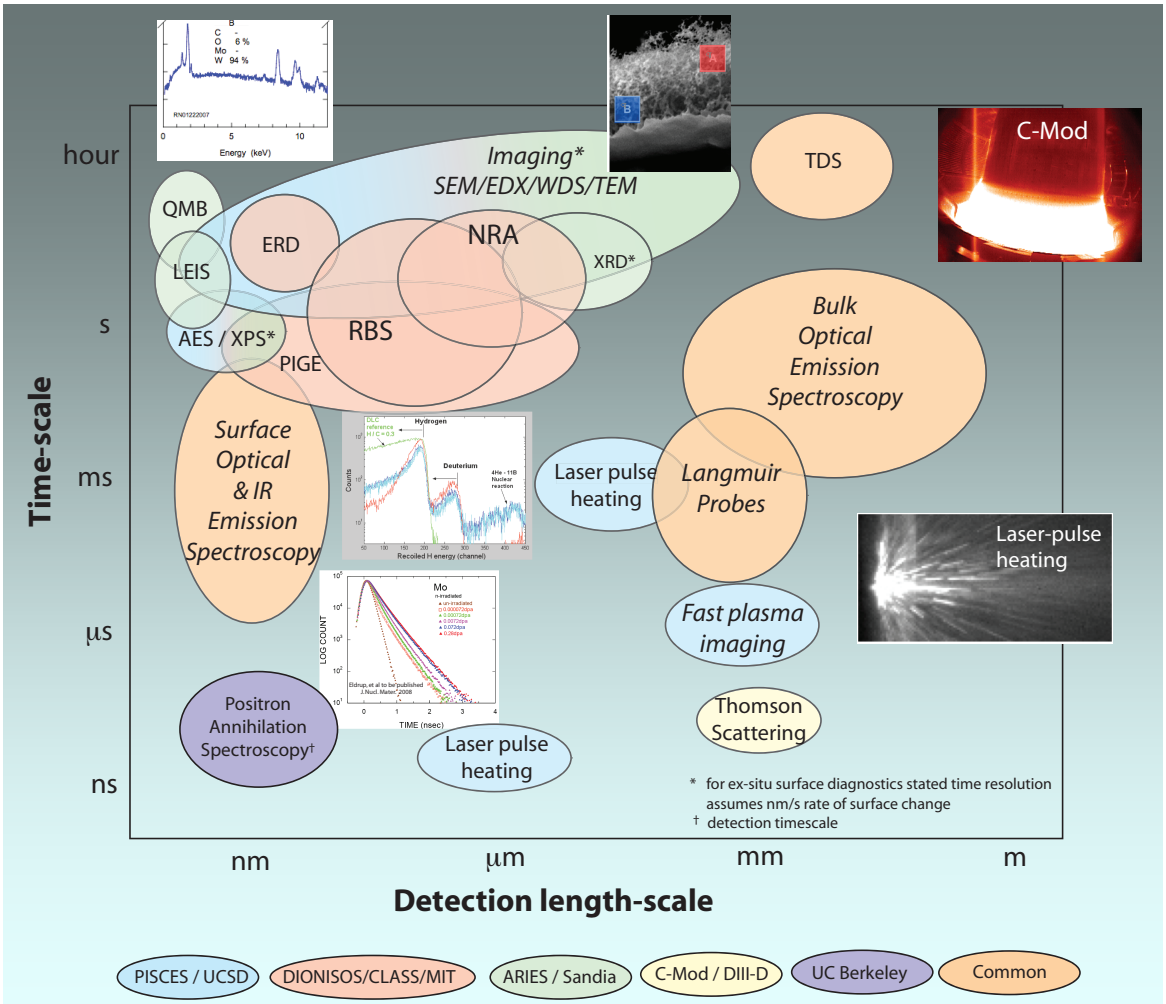

Fig. 4 Multiscale representation of PSI Center surface and plasma diagnostic capabilities.

2.2.1. CLASS & Ion Beam Analysis

The Cambridge Laboratory for Accelerator Study of Surfaces, CLASS, [Wright_AIP11] features a 1.7 MV tandem ion accelerator at MIT and was the Center's workhorse for non-destructive, depth profiled analysis of plasma-exposed surfaces based on MeV ion beam analysis (IBA). The accelerator serves double-duty: ex-situ sample analysis for other Center experiments (e.g. [Chrobak_JNM14, Barnard_JNM11,

Temmerman_JNM13] and the in-situ, real-time surface analysis central to the DIONISOS plasma facility [Wright_RSI14]. We briefly describe the various ion beam analysis techniques available in CLASS/DIONISOS, as highlighted by their acronyms in Fig. 4.

Rutherford Backscattering Spectroscopy (RBS) measures elemental distribution by detecting back-scattered light ions, typically protons or alphas. The depth distribution is inferred from energy spectrum of the back-scattered ions and knowledge of the ion slowing rates. The technique is particularly sensitive to high atomic number elements due to their larger Rutherford cross-section (Fig. 5a–b). Elastic Recoil Detection (ERD) measures forward-scattered elements that are lighter than the beam species. Like RBS, it provides depth profiled elemental distributions. It is typically used with He beams to measure near-surface hydrogenic (H/D/T) or helium profiles with very good depth resolution (< 10 nm). Nuclear Reaction Analysis (NRA) uses exothermic nuclear reactions between the incoming beam and nuclei in the material surface, and is therefore

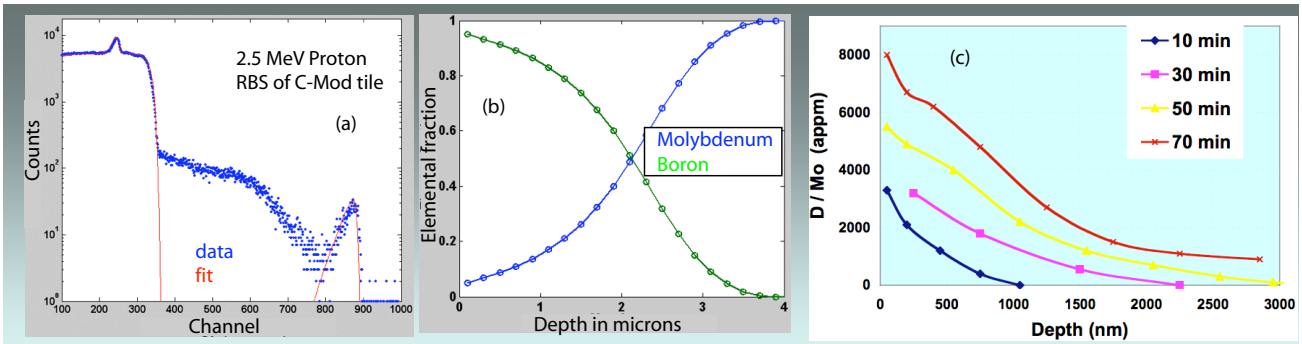

Fig. 5 Examples of ion beam surface analysis. (a) Ex-situ proton RBS spectrum of a boron-coated Mo tile from C-Mod (b) Fitted depth distribution of boron and molybdenum mixed layers (c) In-situ Deuterium depth profiles in Mo at various exposure times to D plasma in DIONISOS using NRA.

particularly well-suited to isotope-sensitive detection. The resulting high-energy nuclear product is detected with charge-particle detectors, and kinematics of the reaction are used to determine depth profiles. An example of NRA deuterium depth profiling, using a 3.5 MeV ^{3}He ion beam, from the DIONISOS experiment is shown in Fig. 5c. The in-situ analysis allows for routine diagnosis of the D permeation through the Mo sample caused by the exposure to the plasma. Particle-Induced Gamma Emission (PIGE) is a subset of NRA which instead detects gamma rays resulting from beam-target nuclear reactions. PIGE has the advantage of being extremely sensitive to wide variety of low-Z isotopes and uses an external gamma detector. Also, certain nuclear reactions that have very narrow energy resonances in their cross-section can be exploited to provide very fine scale (~ nm) depth profiles of isotopes (e.g. H, 13-C) with scanning of the incident beam energy. The CLASS accelerator is particularly well-suited to this with its solid-state charging supply which provides excellent beam energy stability and tuning.

The centerpiece of CLASS is a highly versatile 1.7 MV tandem ion accelerator (Fig. 6). Negative ions are produced at one of two low energy (~30 keV) sources: a sputtering source for most solid materials and protons, and a plasma source for He (alpha) particles. Negative ions are accelerated to the positive terminal ($V_{terminal}$~ 0.05MV-1.7 MV), stripped of electrons through interaction with a controlled N_2 gas leak and then accelerated again to ground potential, thus obtaining ion beam energies up to $(q+1)\cdot V_{terhmial}$. For example the maximum He/alpha ion energy (q=2) would be 5.1 MeV with a 1.7 MV terminal voltage. Terminal voltages up to ~2 MV have been achieved with upgrades to the CLASS insulating gases and internal electronics. The ion beam is focused with quadropole magnets, and mass/energy selected by a dipole electromagnetic, to be finally steered down any of a series of beamlines as a mono-energetic, single species

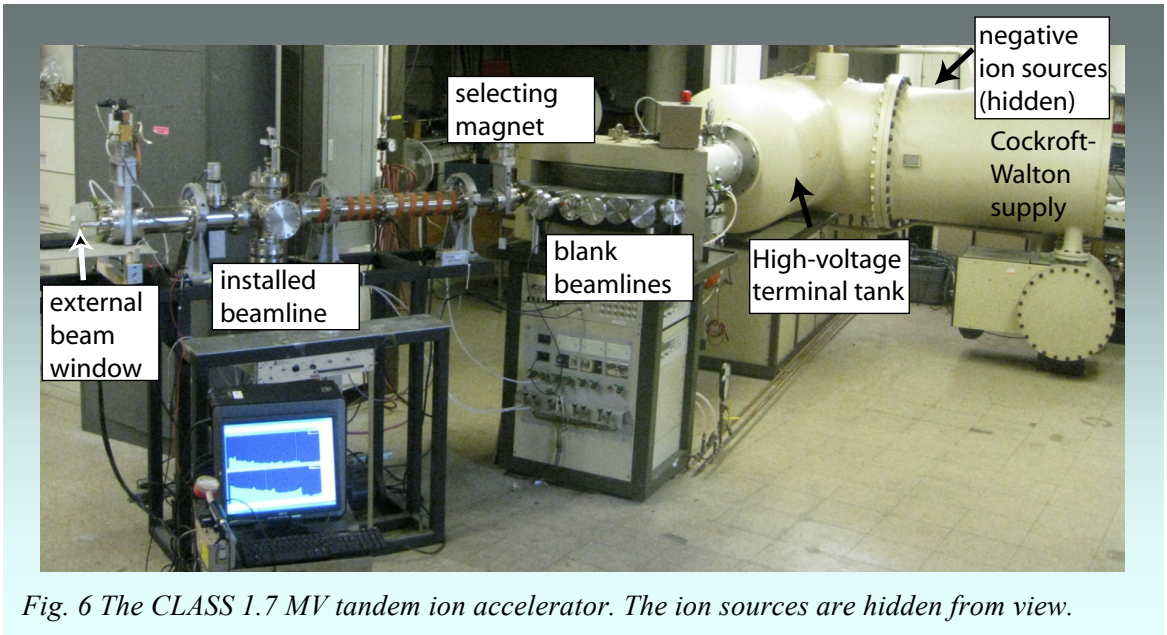

Fig. 6 The CLASS 1.7 MV tandem ion accelerator. The ion sources are hidden from view.

focused ion beam. The dual negative ion sources allow for steady-state ion beam species of nearly any element, with beam currents ~ 1-100 microAmperes, depending on species.

As a Center upgrade we installed a higher performance He negative ion source, using a rubidium charge exchange system, which significantly enhanced the exposure and diagnostic capabilities of CLASS. The terminal voltage is obtained with a solid-state regulated Cockroft-Walton charging supply, which maintains very stable voltage regulation (± 100 V) and provides for straightforward ion beam energy scanning. Upgrades to the Cockroft-Walton improved its reliability and stability at high terminal voltages. Typical beam size diameter is a few mm, and the beam can be electro-statically rastered over larger areas for implantation.

CLASS provides a broad range of material irradiation and diagnosis options, and is also central to the DIONISOS facility (see description below). As a facility for directly exposing materials (Fig. 3), the primary objectives are 1) To implant elemental/isotopic depth markers in material sample for non-destructive erosion analysis [Safo_MS14, Sullivan_NIMB14] and 2) To pre-irradiate materials to intentionally produce deep and distributed damage using the MeV ion beams. Irradiations can also be temperature controlled a variety of sample holders.

2.2.2. DIONISOS

DIONISOS (Dynamics of IONic Implantation and Sputtering on Surfaces) is an experiment dedicated to study the dynamics of plasma-surface interactions, and is one of the keystone experimental facilities of the PSI Center. Its innovative feature as a high-flux plasma PSI experiment is that it is attached to a tandem ion accelerator, which allows for in-situ, real-time ion beam analysis (IBA) of materials at any location on the surface, even during plasma exposures. This compatibility is made possible by the vastly different interaction ranges of the MeV ion beam and the ~eV plasma ions. This capability provides unique non-destructive diagnostic access to the dynamics and depth-resolved evolution of the surface as it is modified by the plasma exposure. The powerful suite of IBA techniques is described in the previous section. Here we describe the plasma and exposure capabilities of DIONISOS.

DIONISOS features a steady-state radio-frequency (RF) helicon plasma driven by a 13.56 MHz RF source [Wright_RSI14]. The source operates in a steady-state solenoid magnetic field up to 1000 Gauss (Fig. 7) and the cylindrical plasma is extracted along the magnetic field into an exposure chamber (Fig. 8). Operating in helicon mode the deuterium plasma flux density up to mid 10^{21} $s^{-1}m^{-2}$ is available (Fig. 3), with higher flux density available for argon and helium plasmas (>10^{22} $s^{-1}m^{-2}$). The RF source can be operated in an inductively coupled mode, which typically decreases the plasma flux by a factor of ten. Plasma electron temperatures are typically ~ 3-10 eV as measured by an insertable Langmuir probe and plasma densities range from ~10^{17}-10^{19} m^{-3}.

The target assembly allows for significant control of exposure conditions. Samples are mechanically attached to a large area (10 cm x 10 cm) copper heat sink, which allows for a wide range of sample sizes and shapes. Externally controlled push/pull heating and cooling of the sample is available from room temperature upwards. A hardware upgrade provided by the Center now allows exposure temperatures up to > 1100 K to better study high temperature fuel desorption, provide in-situ material annealing and better span the temperature range required for tungsten nano-tendril grwoth. The assembly can be rotated 360 degrees, allowing arbitrary angles between the plasma and target.

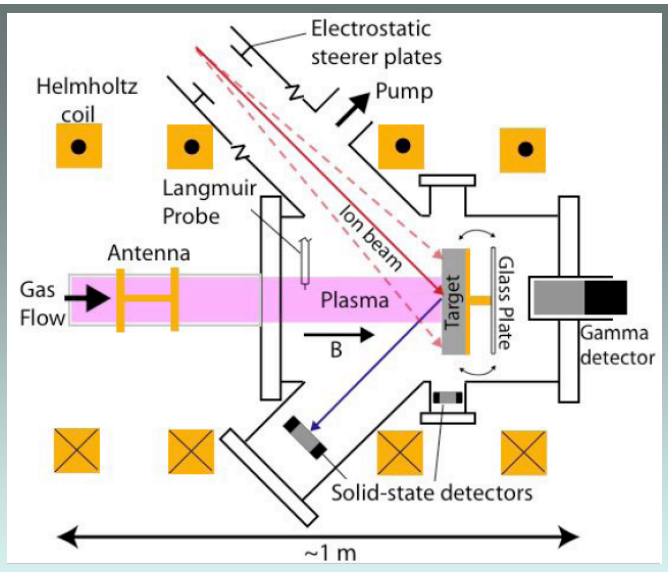

Fig. 7 Schematic of the DIONISOS plasma experiment. The steerable high energy (MeV) ion beam produced by the tandem accelerator allows for in-situ, real-time ion beam analysis of material surfaces undergoing plasma bombardment.

The target is electrically isolated and can be biased to 500 V, allowing for external control of incident plasma ion energy. Samples are readily changed using a large-area rear access door.

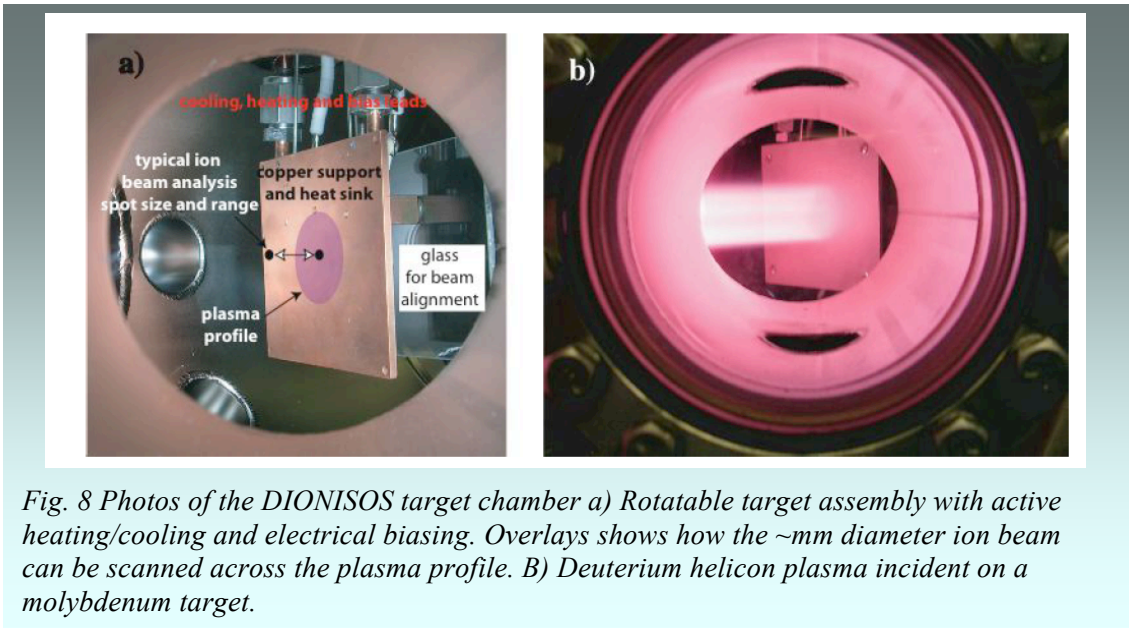

Fig. 8 Photos of the DIONISOS target chamber a) Rotatable target assembly with active heating/cooling and electrical biasing. Overlays shows how the ~mm diameter ion beam can be scanned across the plasma profile. B) Deuterium helicon plasma incident on a molybdenum target.

The DIONISOS facility uses the 1.7 MV accelerator of CLASS. The high-energy ion beam can be brought through to the sample with no physical apertures or occulting, which allows for upstream 2-D electrostatic steering or rastering of the analysis beam across the material surface. The DIONISOS vacuum chamber features a large number (~15) ports with line-of-sight access to the target surface, which provides for excellent diagnostic coverage including charged particle spectroscopy (IBA) and optical coverage (infrared and optical spectroscopy). Specially designed, actively cooled detector housings are used to protect and shield the charge-particle detectors to make them compatible with the plasma environment.

Diagnostic upgrades have been applied to DIONISOS for the Center activities [Wright_RSI14]. New detector clusters with improved electronics were installed for more reliable ion beam analysis. The upstream differential pumping and apertures allowed higher gas densities in the plasma chamber. Active cooling and target shielding also provided for more robust and reliable detector operation.

2.2.3. Alcator C-Mod

_The Alcator C-Mod tokamak is located at MIT Plasma Science and Fusion Center. It is a high-field (B ≤ 9 T), compact (R/a 0.67/0.22 m) tokamak. Plasma heating is carried out with RF in the ion-cyclotron and lower hybrid (LH) frequency ranges, with total heating up to ~ 8 MW, with a particular focus on LH current drive studies. It is unique in the world divertor tokamak program for having only bulk high-Z refractory (molybdenum and tungsten) plasma-facing materials. The combination of high-field compact design

with high power density RF heating means the C-Mod boundary plasma conditions (e.g. plasma density, opacity to impinging neutrals, radiation trapping) match and exceed those of ITER, and in some cases approach those expected in fusion reactors (e.g. parallel power densities in excess of GW/m^2, ion flux densities up to 10^{24} $m^{-2}s^{-1}$), making C-Mod particularly suited to PSI studies and expanded the exposure capabilities of the Center (Fig. 3).

2.3. Research Team & Diversity

A highly capable research team of professional researchers and students was assembled to carry out the research. The MIT members of the team are listed below with their positions and responsibilities noted.

The Center team also strongly contributed to diversity in the field. Two of its members, Sullivan and Kesler, are female. Jude Safo, who graduated with a Master's degree, was an Under-Represented Minority student with an NSF Graduate Research Fellowship.

Dennis Whyte, Professor of Nuclear Science and Engineering.
Served as Principal Investigator and provided academic supervision of students and community outreach.

Graham Wright, Research Scientist, Plasma Science and Fusion Center
Technical leader of the CLASS & DIONISOS facility. Leader of tungsten nano-tendril experiments on Alcator C-Mod and ion beam analysis for DIII-D experiments.

Regina Sullivan, Postdoctoral Associate, Plasma Science and Fusion Center, Research Scientist, MIT Aeronautical/Astronautics Department
PSI diagnostic development. Plasma thrusters.

Harold Barnard, Ph.D. student, Nuclear Science and Engineering
External beam on CLASS.

Kevin Woller, Ph.D. student, Nuclear Science and Engineering
Tungsten nano-tendril and in situ helium diagnosis on DIONISOS.

Jude Safo, M.Sc. student, Nuclear Science and Engineering, NSF Graduate Research Fellow
Depth marker implantation and thermal stability.

Leigh Ann Kesler, Ph.D student, Nuclear Science and Engineering
Anomalous sputter yields on DIONISOS.

Ethan Peterson, B.Sc. student, Nuclear Science and Engineering
DIONISOS in situ erosion yield diagnostic development.

3. Research Highlights

It is infeasible to go into the details of the twenty publications and many presentations resulting from the Center research. Instead here we provide some highlights in selected areas. Please note that the figures are gathered at the end of each sub-section.

3.1. In Situ PSI Diagnostic Development

A central theme of the MIT effort in the PSI Center was the development of new and exciting diagnostic capabilities. A particular focus was placed on in situ diagnosis, i.e. the ability to make measurement of surface evolution in place.

The DIONISOS experiment is shown in Fig. 9 with full upgrades installed for the Center research. The plasma and ion beam analysis can be operated continuously and simultaneously. All key components have active cooling for steady-state operation. The material sample has push-pull temperature control independent of the plasma heat flux which provides the needed sample material temperature control which is critical to conducting material exposure experiments. The response of materials is highly sensitive to material temperature. Thus DIONISOS provides unparalleled capabilities to study the modification and dynamic response of a material surface to the presence of a high intensity plasma.

An extensive benchmarking exercise was undertaken with the upgraded DIONISOS to both develop in situ measurement techniques of the surfaces, and to validate the ion beam analysis results [Wright_RSI14]. This validation exercise is motivated by the fact that the DIONISOS/plasma environment is highly unusual and demanding for performing ion beam analysis. For example, Fig. 10 shows that the gas and magnetic field of the DIONISOS environment do not affect the accuracy of Rutherford Backscattering Spectroscopy ion beam analysis. IBA provides depth-resolved measurements over < 10 microns. Therefore, the samples must be prepared with "features" to distinguish the removal or addition of material on samples. In order to demonstrate the ability to make in situ erosion measurements, aluminum samples were coated with 1.6 micron layers of copper. The resulting in situ RBS data is shown in Fig. 11. The copper backscatters at higher energy due to its larger mass. When the copper layer thickness and the RBS are appropriately designed the copper shows up as a distinct "rectangle" in the backscatter spectrum. This requires care in the RBS design in particular because of the limited geometry allowed for the detectors in the presence of the plasma. As the copper thickness recedes, or grows, this is apparent in the RBS spectrum and thus erosion/deposition is measured. It is also possible to measure any material mixing or inter-diffusion.

The RBS spectra are then taken sequentially with the plasma bombarding and the changes from spectra to spectra are fit and interpreted as erosion rates. An example of such a measurement is shown in Fig. 12. *It is clear that the erosion rate is in fact not*

constant through time, with the erosion rate being larger at the beginning of the sample exposure. This feature is generally found for samples [Peterson_SB13]. Note that in "cook and look" experiments it must be implicitly assumed that erosion is constant. *This ability to quantitatively measure the surface evolution, in order to correctly interpret the dynamic response of the material, is at the heart of DIONISOS*.

In addition to erosion and deposition rates of the surfaces, DIONISOS can also use IBA to determine the concentration of the plasma species. An example of this is shown in Fig. 13 for the retention of deuterium in refractory metal. Using 3-He NRA the depth profile of the deuterium is tracked as the controlling parameters of the deuterium transport are changed (e.g. D fluence, material temperature.) yet while the plasma is in contact with the material. The high-flux plasma environment "forces" the deuterium into high concentrations well past those expected from solubility calculations. Dynamics are important to the plasma-species and material interaction; for example the deuterium content transiently increases under plasma loading. The ion beam of DIONISOS can also be used to alter the material properties. Fig. 14 shows that the displacement damage caused prolonged ion beam exposure can strongly enhance the deuterium retention [Wright_RSI14]. This is caused by the production of defect sites that can "trap" the deuterium atoms.

It is critical to develop robust methods to measure the net erosion and deposition rates of plasma-facing materials. In the example described above, the copper erosion is measured by "artificially" producing a copper film that can be followed by IBA. So while this is a powerful surface measurement tool, it would be more desirable to study a bulk material's erosion. This requires a "depth marker", i.e. some species which is distributed in the material and its apparent depth tracked. The PSI Center has developed an exciting new depth marker technique. Most depth markers use a high-Z tracer because this can be easily measured by elastic scattering (e.g. RBS) due to its high cross-section. However this is inappropriate for high-Z materials, plus it is harder to implant the high-Z marker deep into the material. Thus we have developed a novel lithium depth marker [Sullivan_NIMB14]. High-energy lithium (~6 MeV) ions are implanted into the plasma-facing material to a peak local atomic concentration of ~5% Lithium is beneficial in three ways: 1) it has high penetration into the material due to its low mass 2) it creates nearly the minimum amount of damage in the bulk material and e) it exhibits a very high Q~19 MeV cross-section with protons producing two alphas. Thus an even more penetrating proton ion beam (2-3 MeV) is then used to probe the depth of the implanted lithium layer by measuring the energy spectrum of the alphas from the p-^{7}Li reaction. The alphas have such high birth energy (~10 MeV) they readily penetrate back to the surface, yet their detected energy is modified by the amount of material between the lithium layer and the surface (Fig. 15). Thus if the alpha energy shifts this indicates erosion (if the alpha energy upshifts) or deposition (alpha energy downshifts). The Gaussian energy distribution is the result of the lithium spatial distribution in the material due to straggling; thus the lithium's diffusion in the material can also be monitored. Due to the exploitation of very high-Q nuclear reaction the technique has very high linearity and dynamic range, making it almost an ideal depth marker (Fig. 16). The surface composition can also be monitored using standard RBS from elastic proton scattering

which can be obtained simultaneously with the depth-marker diagnosis. The new lithium depth marker was shown to be highly accurate in determining the erosion rate of aluminum by argon ions, which has a well-known experimental sputter yield. Fig. 17 summarizes the erosion test results while Fig. 18 shows experimental pulse height energy spectra of the alphas produced by the proton probe. Besides the IBA advantages provided by the 7-Li, this demonstration shows that the implantation of the lithium is essentially non-perturbing to the plasma-facing material properties. This makes the lithium depth marker more appropriate than films for the harsh thermal environment encountered in fusion plasma and plasma thruster applications.

An examination of Fig. 18 shows that the Gaussian width of the alpha spectrum is unmodified by the plasma exposure. This indicates a stable lithium distribution in the aluminum bulk material. However in a high temperature environment one may expect that the Gaussian distribution of the lithium will spread out through thermally induced diffusion. This diffusion would make the lithium average depth less "sharp" and thus degrade the depth marker and erosion resolution. Aluminum, while convenient for initial tests, is not a common plasma-facing material. Therefore the use of the lithium marker was tested in a more realistic environment [Sullivan_NIMB15]. Lithium was implanted into boron nitride samples and heated to very high temperatures (Fig. 19). Boron nitride is a very common plasma-facing material in plasma thrusters. Despite ~hour long heating of the samples to > 1000 K the experiments found no measurable diffusion of the depth marker (Fig. 19). This implies that the lithium is residing in extremely deep energy trap sites in the BN and is thus highly resistant to thermal diffusion. In addition we have tested the thermal stability of high-Z gold depth markers in refractory metals and have also shown these are extremely resistant against thermal diffusion as shown in a recent Master's thesis[Safo_MS14]. These results are highly favorable for application of the lithium depth marker technique to realistic erosion/deposition studies in fusion and plasma thrusters where elevated temperatures are expected. Research is presently underway to implement the lithium marker in both tokamaks and magnetized-cusp plasma thrusters.

The depth marker technique has also been used to discover unexpected sputtering behavior. Using exactly the same lithium depth marker implanted into aluminum, when the plasma species is switched from argon to helium, the measured sputter rate decreases dramatically compared to the predicted rate. The measured pulse height spectra are shown in Fig. 20 from these experiments. The measured erosion rate is ~680 nm, however this is more than ten time less than expected from the sputter yield of He on aluminum at 100 eV and the measure He ion flux. Calculations show that this decrease in net erosion cannot be caused by redeposition of the aluminum back onto the target; i.e. the mean free path for ionization was kept intentionally longer than the plasma radius. This measurement confirmed the same trends of anomalously low sputter yield as seen for helium plasma on certain metals in PISCES. The PISCES results were obtained with mass loss. Thus two independent measurement techniques verify that for high flux-density He plasmas the sputter yield of certain metals can be made much lower than expected from the Binary-Collision Approximation sputter models. The reason for this anomalously low sputter yield is presently under investigation. The observation that the

BCA model is becoming invalid indicates that the reason must be the dynamic response of the surface composition due to the presence of the high flux density plasma; this effect is not seen for low flux density ion beams for instance. Thus DIONISOS is the ideal experiment in which to study this intriguing behavior: and understanding how can the dynamic sputter yield of materials be decreased is of great practical interest. This topic was to be the Ph.D. thesis of Leigh Ann Kesler (Sec. 2.3) but is presently unfunded due to the closure of the Center.

The Center was also involved in advancing low temperature plasma diagnostics. The focus of this was the use of Ion Sensitive Probes (ISP). These are a broad class of electrostatic probes for use in magnetized plasmas. The basic feature (Fig. 21) of the ISP is that it uses the large difference in ion and electron gyroradius to allow ions to enter into a recessed volume yet shield direct electron entry. Charged particle current is measured versus applied voltages on the "collector" which is at the bottom of the ISP and on an electrically isolated "wall" of the probe. Previous work on DIONISOS had shown that the standard interpretation of the ISP was incorrect and that the key observation was that charge particle collection had to terminate when the wall voltage was elevated above the plasma potential. In this way the ISP can be used as a cold plasma potential probe; which is a critical measurement for PSI since the plasma potential largely determines the incident ion energy and sputtering. The ISP probes were then deployed in confinement experiments to measure in particular the increased plasma potential due to RF heating. The previous DIONISOS research had hinted at internal dynamics within the probe volume setting the physics of the ion collection. This was verified by Center research on DIONISO [Sullivan_JNM13] where the collector was physically split into independent probes. The results of the experiment are shown in Fig. 21. As the fixed bias between the wall and collector was changed the asymmetry in charged particle collection also varied. This showed for the first time that ExB drifts were dominating the internal dynamics of the ISP, along with space-charge effects. This insight was critical to understanding the interpretation of ISP in the much higher density of the C-Mod edge plasma. The ISP was deployed in C-Mod based on the DIONISOS work [Brunner_RSI13] and it was determined that space-charge effects were dominating the attempts to use it to measure ion temperature [Brunner_PPCF13]. This clearly indicated that the interpretation of ISP traces in other experiments has been incorrect with respect to ion temperature. At the same time the ISP proved to be a very robust measurement tool for the plasma potential and thus PSI experiments in the confinement devices. This is one example of how Center diagnostic research made a broad impact on the boundary plasma and PSI fields.

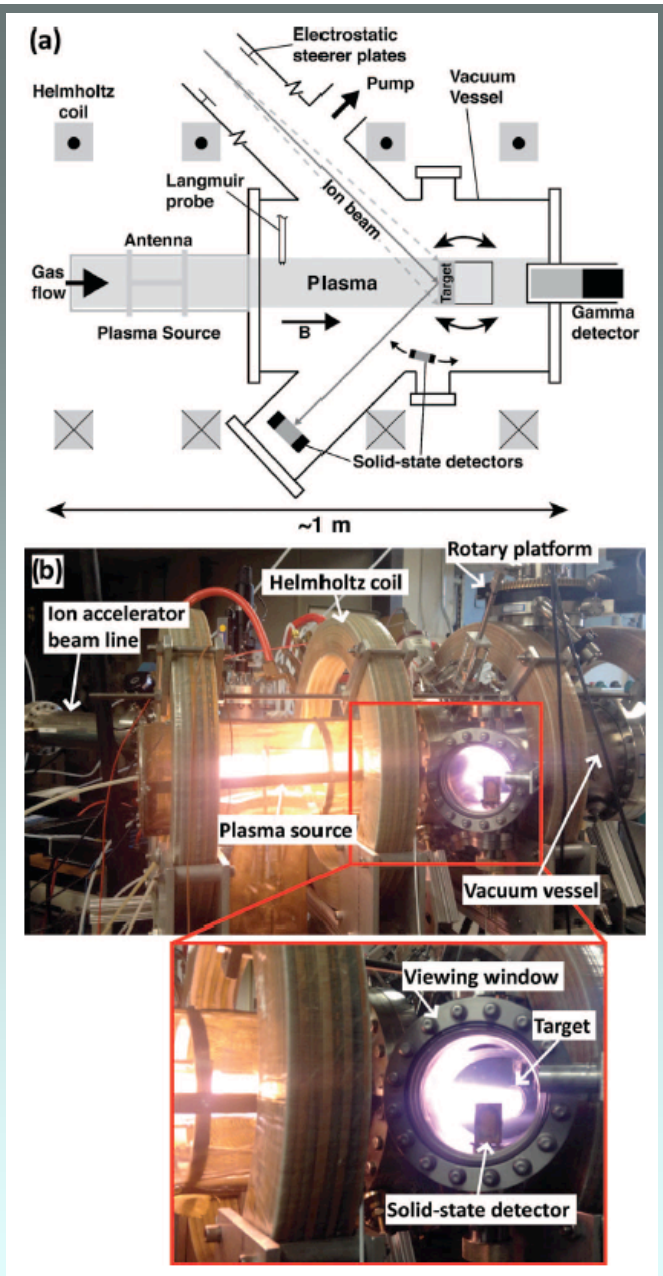

Fig. 9 (a) Schematic of the DIONISOS experiment (b) Photos of DIONISOS in operation [Wright_RSI14]

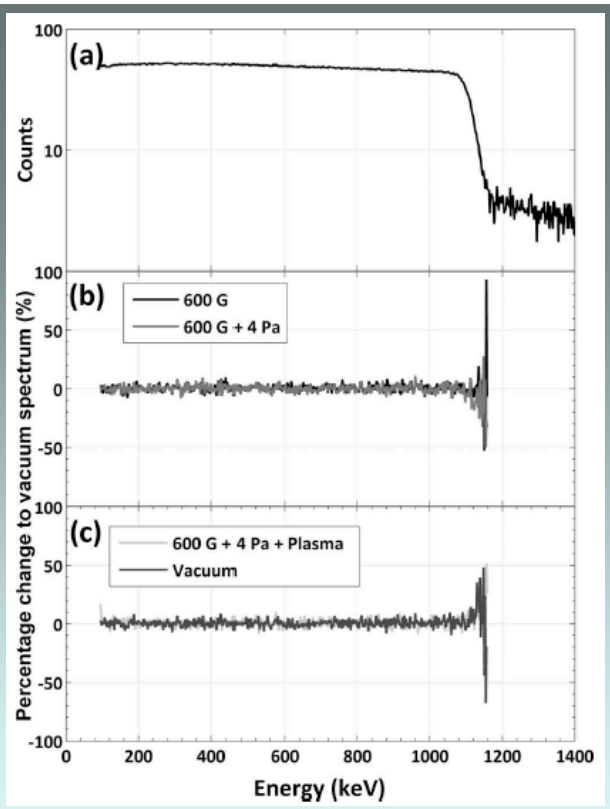

Fig. 10 (a) RBS spectrum of 1.2 MeV protons off W target in pure vacuum.(b) The percentage change induced in the spectrum by introduction of a 600 G axial magnetic field and a 600 G field plus 4 Pa of background He neutral gas.(c) The percent change induced in the RBS spectrum by the introduction of 600 G magnetic field, 4 Pa of neutral He pressure, and a He plasma incident on the target; and the percent change in a second spectrum taken in vacuum is also shown to demonstrate the natural variability in the spectra. [Wright_RSI14]

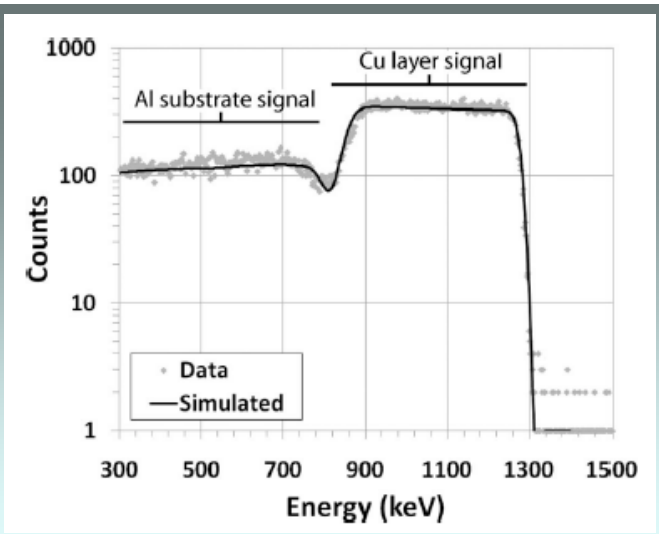

Fig. 11 An RBS spectrum in DIONISOS for a 1.6 μm Cu layer deposited on an Al substrate as measured by 1.4 MeV protons. simNRA produces the numerical simulation [Wright_RSI14]

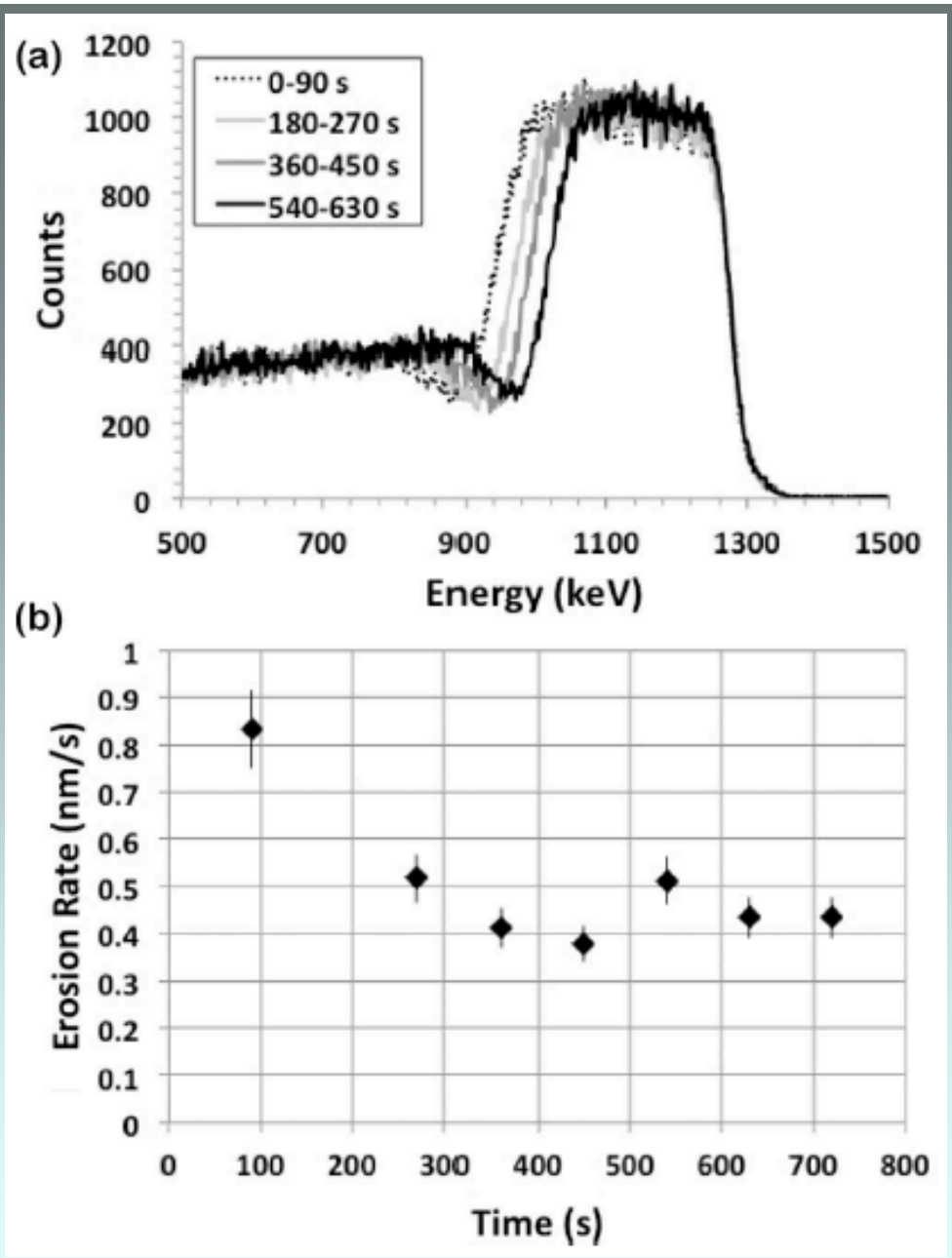

Fig. 12 (a) A series of RBS spectra during an exposure of 1.6 μm Cu (copper) layer target to He plasma in DIONISOS. The times refer to the time of the plasma exposure over which the respective spectrum was collected. (b) The corresponding Cu erosion rates calculated by simNRA simulations of the Cu thickness in sequential RBS spectra [Wright RSI14].

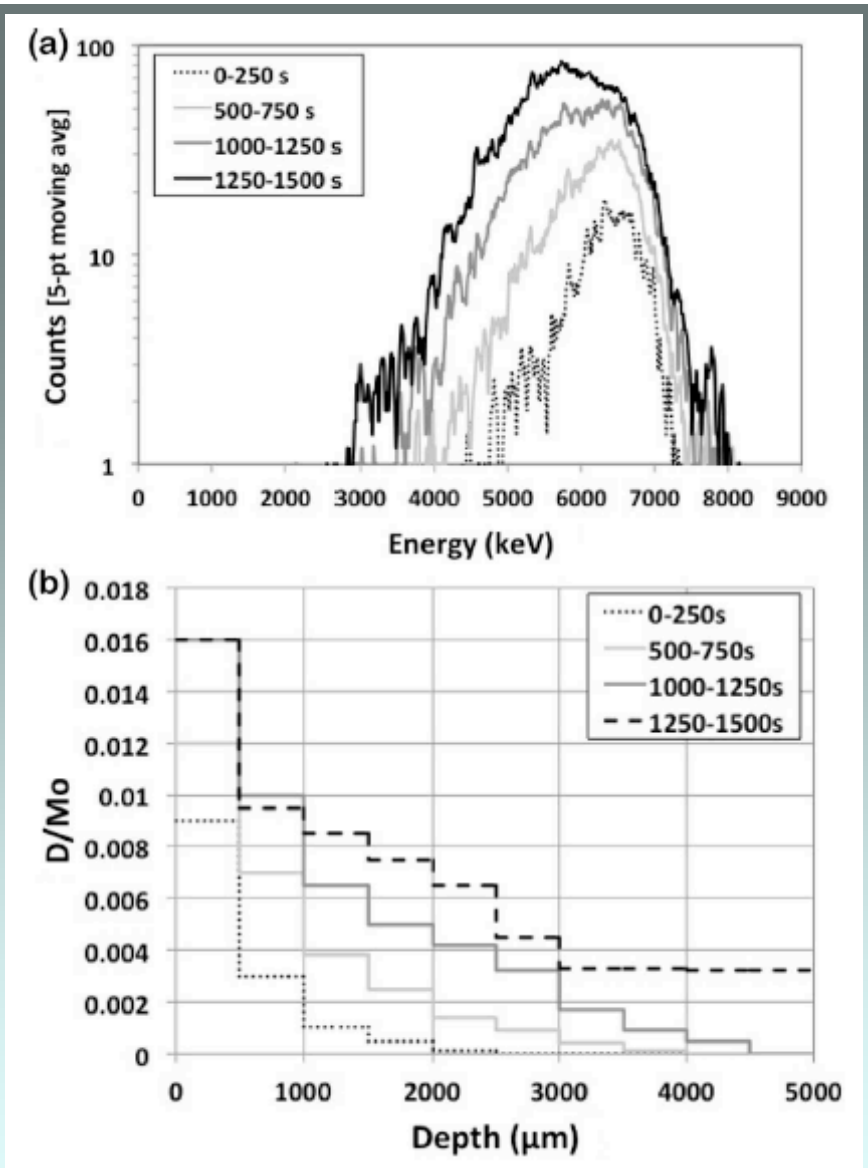

Fig. 13 (a) A series of Nuclear Reaction Analysis (NRA) spectra measuring the Deuterium fuel content in a molybdenum high-Z target at 400 K exposed to D plasma. The counts are plotted as a 5-point moving average for clarity. (b) The corresponding D depth profiles to the energy spectra in (a) as determined by simNRA fits [Wright_RSI14].

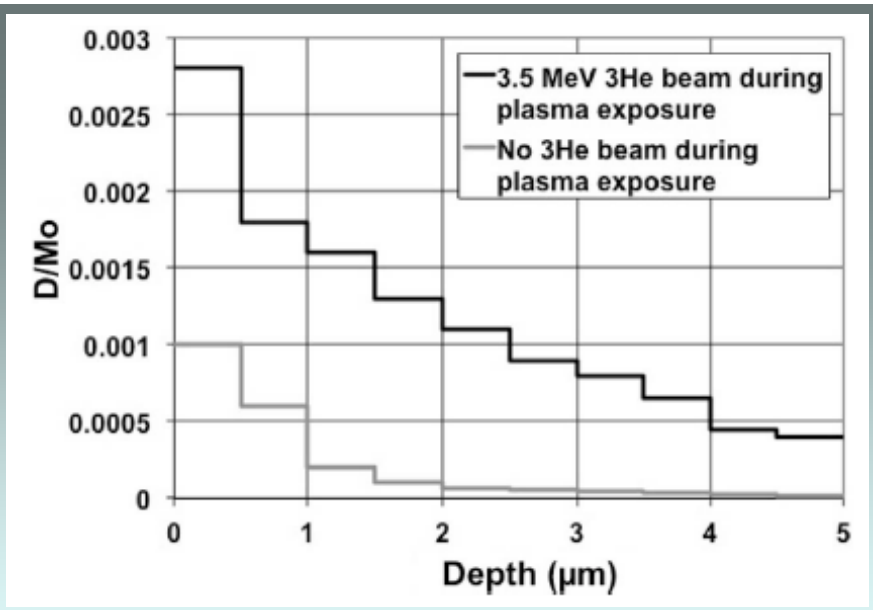

Fig. 14 A comparison of the Deuterium content in a high-Z Mo target exposed to Deuterium plasma with and without the 3.5 MeV 3He++ bombarding the surface, demonstrating the significant impact of the ion beam on the experimental results. [Wright_RSI14]

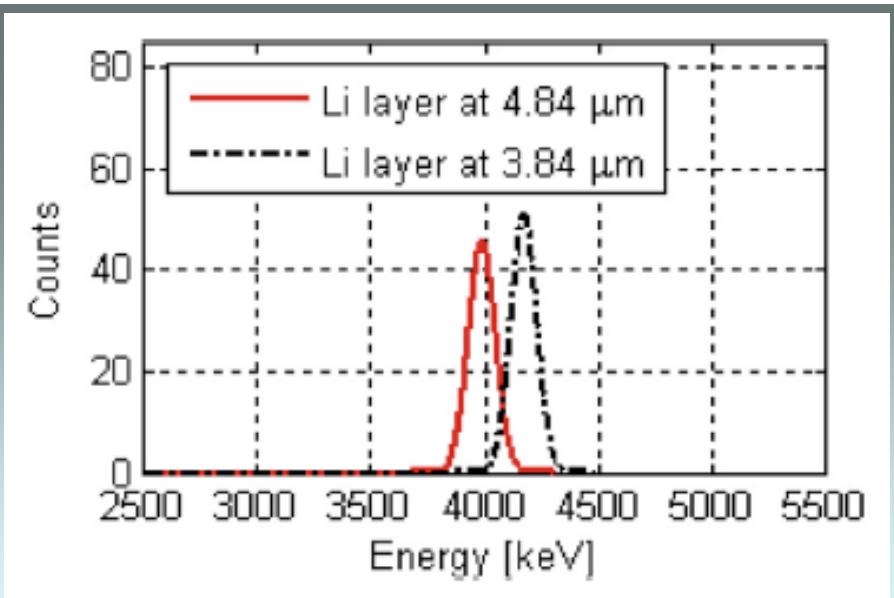

Fig. 15 Simulated erosion in simNRA using the lithium depth marker technique. Simulated erosion of 1 microns from the original implantation depth of 4.84 micron is shown. The corresponding upshift in energy of the alpha peak is 185 keV after erosion. [Sullivan_NIMB14]

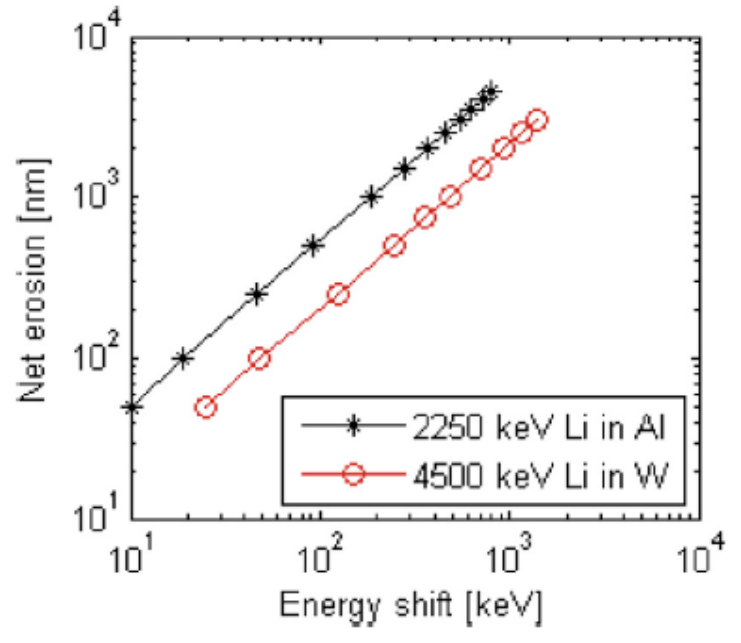

Fig. 16 Net erosion vs. shift in energy of the alpha peak generated by the ^{7}Li-proton reaction, as calculated using SIMNRA. The Aluminum data corresponds to a layer implanted with a 2250 keV Li beam, and the W data corresponds to a layer implanted with a 4500 keV Li beam. The simulation results show the lithium depth marker technique has high linearity and a large dynamic range. [Sullivan_NIMB14]

Simulated sputter yield data, Ar on Al.

Bias voltage (V)	Ion energy (eV)	Sputter yield (atoms/ion)
0	12	0.0
−25	37	0.0098
−50	62	0.045
−75	87	0.096
−100	112	0.13

Case	ΔE_{exp} (keV)	Δd_{exp} (atoms/cm^2)	Δd_{exp} (μm)	Δd_{pred} (atoms/cm^2)	Δd_{pred} (μm)
E0	−16	5.02×10^{17}	0.08	0.00	0.00
E1	357	-1.19×10^{19}	1.98	-1.10×10^{19}	1.83
E2	625	-2.09×10^{19}	3.49	-2.20×10^{19}	3.66

Fig. 17 Summary of erosion result for Argon plasma ions on aluminum (top) Exposure sample biases in DIONISOS and BCA model approximations for sputter yield. B) Comparison of experiment ('exp') and predicted ('pred') atomic density and depth eroded for different sample histories. The depth marker determination of erosion is in excellent agreement with prediction. [Sullivan_NIMB14]

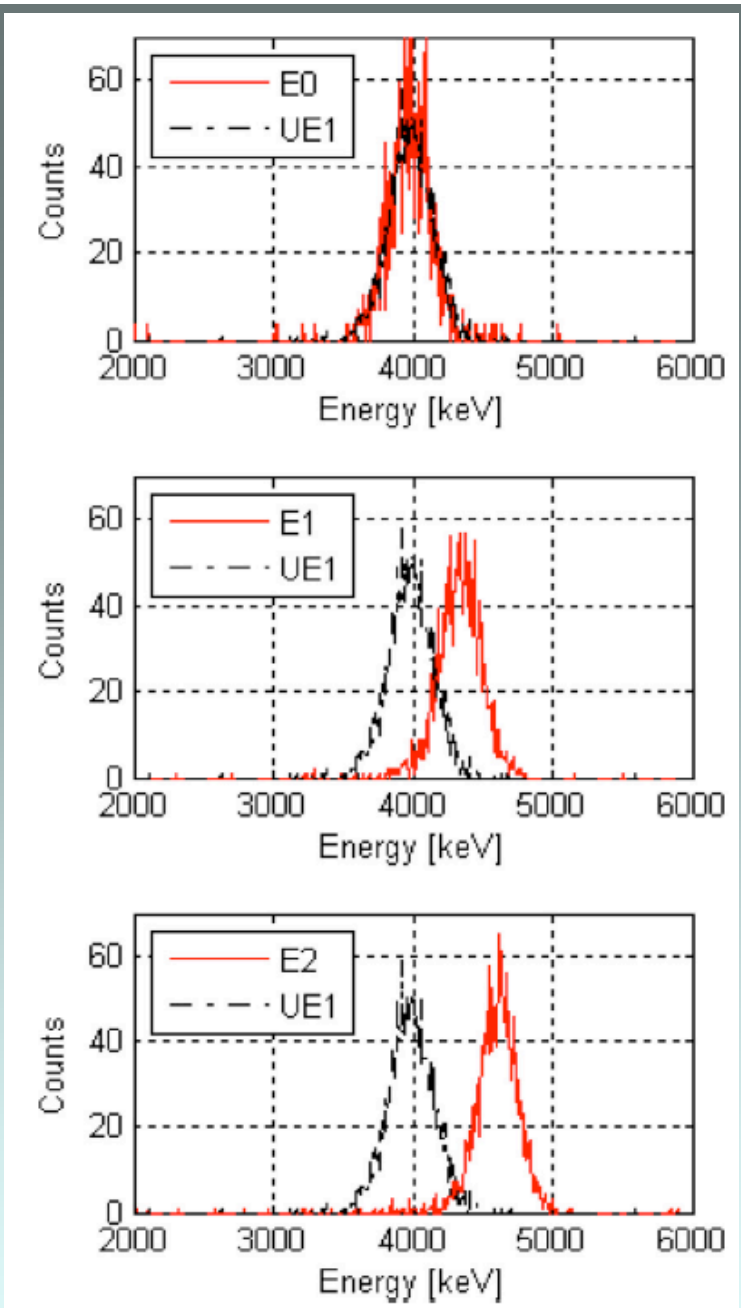

Fig. 18 Experimental profiles for the lithium depth marker [Sullivan_NIMB14]. Calibrated Pulse height energy spectra are shown for the alpha particles produced the proton-^{7}Li reaction from the depth marker. UE: unexposed. E0 was a 30 minute exposure at floating potential which produced no measurable erosion. E1 and E2 are for progressively longer exposures and the increase in the alpha peak is evident as the sample is eroded (Fig. 17)

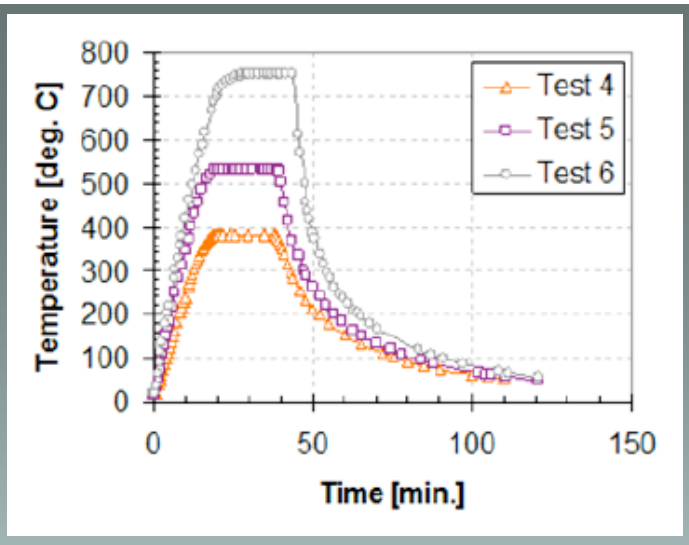

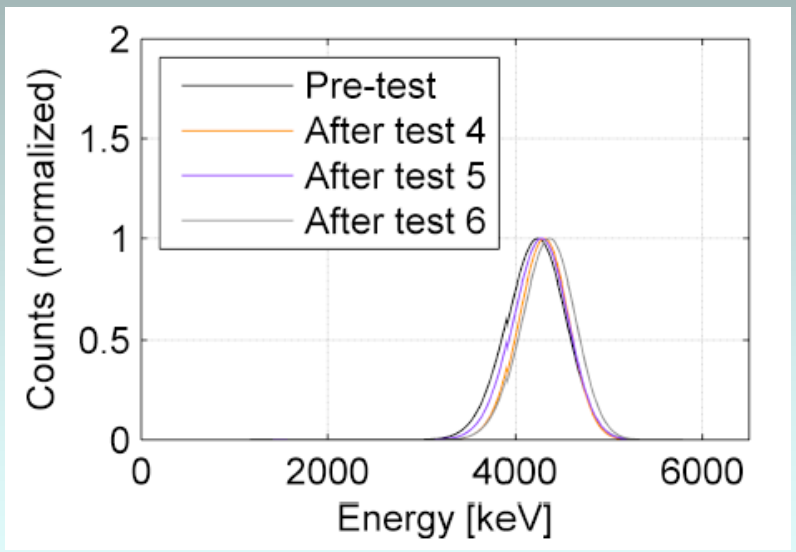

Fig. 19 Test of the thermal stability of the lithium depth marker [Sullivan_NIMB15] (Top) Exposure history for three boron nitride sample implanted with a depth marker (Bottom) The NRA spectra from the lithium are un-broadened indicating the lithium depth marker is highly stable in the BN.

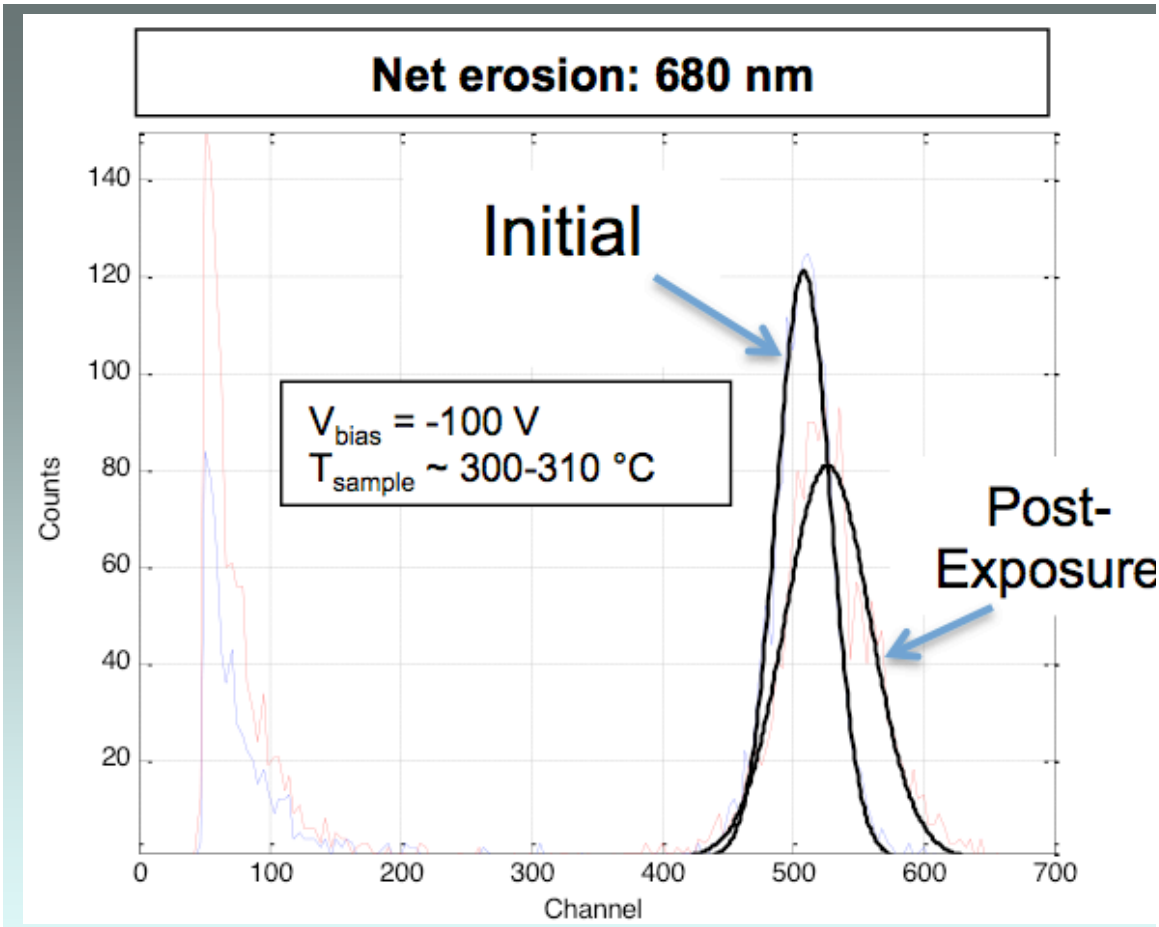

Fig. 20 Lithium depth marker measurement of net erosion of aluminum after exposure to a helium plasma in DIONISOS. The change in the pulse height peak location indicates 680 nm of erosion of the aluminum. However the predicted amount of erosion from a calculated sputter yield of 100 eV He on aluminum is over 10x larger than 680 nm. This indicates an anomalous low sputter yield for high-density He plasma on aluminum.

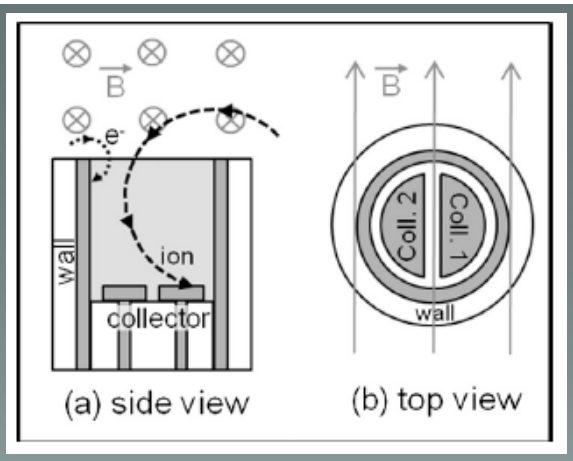

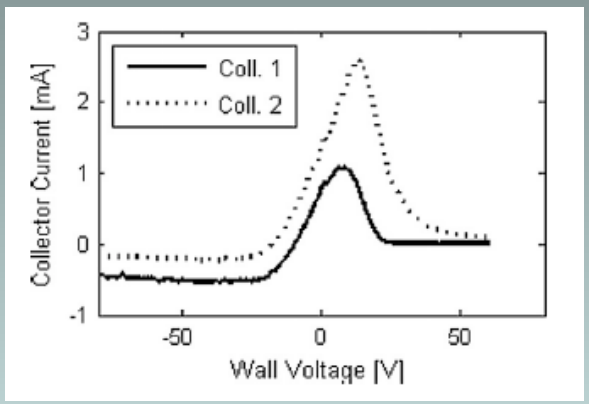

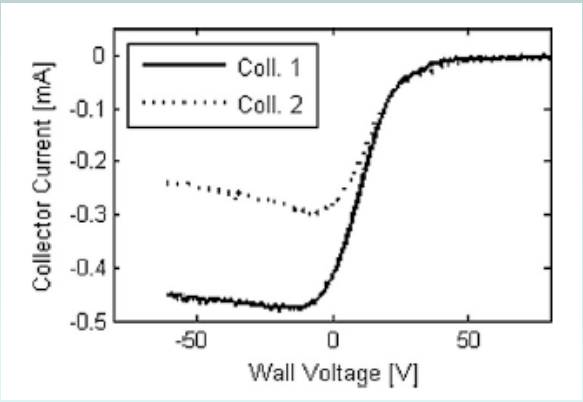

Fig. 21 Test of the Ion Sensitive Probe (ISP) in DIONISOS. (top) The geometry of the probe, magnetic field and particle orbits are shown from the side and top (middle) I–V curve for Case 1 ($V_{wall} = V_{collector}$ - 10 V). Current measured on the two halves of the collector, as the wall voltage is swept from -80 to +60 V. Positive current is net electron current. ExB drift due to the applied electric field would tend to push particles toward Coll. 2 as shown (bottom) Same as middle except for $V_{wall} = V_{collector}$ + 10 V) which disallows electron collection. In this case the ExB drift tends to push particles toward Coll.1 which is seen to have more current than Coll. 2.

3.2. In situ studies of helium-induced nano-tendrils in tungsten

The spontaneous growth of refractory metal nano-tendrils (commonly called "fuzz") from surfaces exposed to helium plasmas has been one of the most interesting developments in PSI in the last decade. Besides the highly intriguing science behind this self-organization in an extreme environment, the strong deformation of the surface of tungsten could have great practical importance since it is the leading candidate plasma-facing material due to its sputtering resistance. The small-diameter (~10-20 nm) tendrils grow from the tungsten when the surface is exposed to sufficiently high flux density of helium ions and temperatures between 1000K and 1800 K. These conditions are likely in ITER and future fusion devices with high-temperature metal divertors. The tendrils grow at varying rates but have been produced up to the ~10 micron depth. These raise concerns because if the tendrils become unstable and breakoff then they can compromise the erosion resistance of the tungsten, and also produce large quantities of tungsten dust into the divertor and plasma. Helium will be intrinsically present in all fusion devices because it the ash particle of the D-T fusion reaction. However the underlying cause of the tendril growth has remained uncertain. Likewise, means of mitigating the tendrils have not been developed. The tendrils represent an obvious strong cross-interaction between the plasma and the surface. Therefore it is highly amenable to in situ inspection using the DIONISOS device.

Helium implantation at high flux density is the starting point for the tendril growth. The growth of nano-tendrils in refractory metals seems to be only associated with helium, not other plasma species. Helium is insoluble in metals and therefore tends to precipitate in void and bubbles. Therefore it is natural that we applied the surface diagnostic tools of DIONISOS to determine the helium content of the tungsten nano-tendrils. Helium is very difficult to measure in materials due to its low Z and it chemical inactivity . In DIONISOS we have applied Elastic Recoil Detection (Fig. 22) using high-energy oxygen beams. The oxygen ions forward recoil the helium in the material surface and are detected in a charge-particle detector with a range foil that stops the deflected oxygen ions. The energy spectrum of the scattered He can be reproduced into a depth-resolved atomic density and concentration of the helium; and this is obtained non-destructively [Woller_JNM13]. The setup is experimentally challenging due to the sensitivity to the grazing angle of the beam and noisy plasma environment. However those obstacles were overcome to produce quantitative helium depth profiles [Wright_RSI14].

The general feature of helium in the tendrils is shown in Fig. 23. The "fuzz" is a complex, randomized structure of the tendrils growing from the tungsten surface (these are pure W). The ERD spectrum clearly shows a high energy plateau caused by the implanted helium in the fuzz. The spectra taken of fuzz always have this feature: namely constant high helium concentration which is very close to uniform throughout the fuzz depth. It is important to note that the "depth" resolution is really an energy resolution set by the ion slowing rate in the materials. Through simulation reconstructions the atomic concentration of helium to tungsten is quantified as a function of effective depth through

the material. The results of studying fuzz with ex situ ERF from linear plasma devices is summarized in Fig. 24. The interesting trend is that the helium concentration is highly constant in the fuzz with values being typically He/W ~ 2-3 %. Although tendril growth is highly dependent on temperature, the helium concentration does not vary much at the low temperature boundary between non-fuzz and fuzz samples. The helium fraction is never above 5% and only falls well below 1% for exposure temperatures above 2000K, which is above the W recrystallization temperature, where no fuzz grows. This suggests highly stable helium bubbles in the fuzz which require very high temperatures to depopulate, since the solubility is nearly zero for helium in tungsten.

While ~2% is a high concentration, certain numerical and analytic modeling indicated that such a concentration is insufficient to create the tendrils. In these models, the tendrils are assumed to be the result of very high pressure helium in the voids which can lead to distortion of the W surface when the helium gas pressure exceeds the yield stress of tungsten. Modeling showed that with helium atomic concentrations He/W~40-50%, and a helium bubble size in agreement with experiments, that the tungsten should distort. This seems like a strong candidate for the tendril growth. However in order to test this idea, in situ measurements were needed in DIONISOS.

A series of experiments was carried out in DIONISOS to grow W fuzz while simultaneously monitoring the Helium depth profile [Woller_JNM14]. The experiments varied the incident He flux density and tungsten temperature. The exposure conditions and SEM micrographs of the surfaces are shown in Fig. 25 showing obvious tendril growth in some cases, and the absence of tendrils in others. Note that is in other experiments the tendril growth is present only above ~1000 K. The results of time-resolved situ ERD measurements of helium concentration are summarized in Fig. 26 for samples that grew fuzz and in Fig. 27 for samples without fuzz. The immediate realization is that the steady-state level of helium concentration is ~ 3-5 % He/W and there is little variability between fuzz and non-fuzz samples. This observation determines that simple distortion of the tungsten through gas pressure cannot be the cause of the tendril growth: the helium concentrations and pressure, *while the fuzz is growing,* is an order of magnitude too small. The ERD also shows the time evolution of the helium and tungsten fuzz. The helium concentration takes ~100 s to build up and the reaches an equilibrium. This is an extraordinary long time scale at the atomistic level. Once this level is reached near the surface, which would indicate the saturation of helium bubbles close to the surface, the tendrils start to grow as indicated by the He and W fluence which are proportional to the tendril height (Fig. 26). The tendrils grow with the square root of time, in agreement with other experiments, whereas in the low temperature cases the saturated high He density bubbles form at the surface but no further growth is seen after ~200 s. It is clear from these results that there is no "threshold" value of helium concentration to induce the tendril growth. It also shows the great power of in situ ERD measurements which allow one to continually monitor the tendrils (or lack thereof) without the need for intervention into the plasma chamber to retrieve the sample. In this way much more information can be obtained in single experiments. A particular example of this is the comparison between the "c" cases of low flux and high flux. The ERD clearly shows that the low flux case does not produce tendril growth despite the 1100 K temperature. This is

a strong indicator of how the helium arrival rate, and not necessarily the He concentration, is a controlling factor in tendril growth.

Given that the leading model for tendril growth was eliminated by the ERD measurements in DIONISOS, it is obviously necessary to search for the cause of the growth. This has taken a major leap forward by the observation of a new form of tendrils [Woller_PhD15]. In certain cases of exposure, the central part of the sample, where the incident He flux density is highest, seemed to lack tungsten fuzz because they were not optically black (optical absorption is a feature of uniformly distributed fuzz as seen in the micrograph of Fig. 25 because they are effective light traps at visible wavelengths).

These central "bare spots" were mysterious since the temperature and flux density conditions were appropriate for growing the tendrils, and the ERD showed that high helium content was present. However on closer inspection with SEM in fact there were tungsten nano-tendrils but there were not evenly distributed on the surface (Fig. 26). Rather the nano-tendrils appear in large "haystacks", i.e. the tendrils are accumulated in a small fraction (<10% of the sample's surface area) while the remaining surrounding surfaces show no distortion. This explains the optical reflectivity of these "bare spots" but they are not bare at all. Indeed a survey of these haystacks show that the total volume of nano-tendrils in these areas is equivalent to the volume where the surfaces are optically black. Therefore the haystacks are typically 10 times higher than the uniformly grown fuzz found on the same sample, but only cover ~10% of the surface. Local FIB was also used to cross-section the haystacks. It is clear that these haystacks are growing from the original surface: i.e. no apparent "hole" was being dug into the tungsten below the haystack. *These amazing tendril features clearly indicate that the origin of the tungsten atoms in the tendrils must arrive by surface transport of tungsten atoms from other locations on the surface.* These are almost certainly adatoms moving on the tungsten surface and, for some reason, forming the tendrils in single locations on the surface. This fundamental insight is critical to understanding and controlling the fuzz growth mechanisms. Further analysis and experiments are presently underway to understand the helium flux density and material temperature dependencies on the tendril growth. A preliminary result is that the tendril growth is sensitive to grain orientation: a result which is consistent with varying activation energies for adatoms. This research constitutes the Ph.D. work of Kevin Woller [Woller_PhD15].

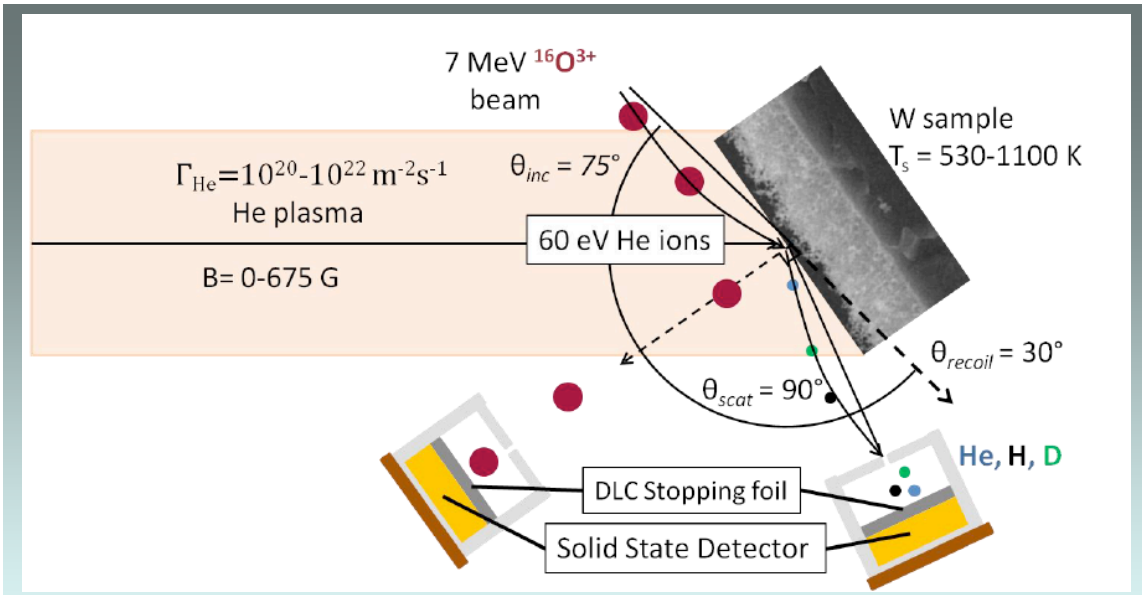

Fig. 22 Schematic of in situ ERD and RBS measurement for real-time monitoring of tungsten nano-tendrils in DIONISOS during He plasma exposure. The 7 MeV oxygen ion beam is provided by the CLASS accelerator [Woller_JNM14]

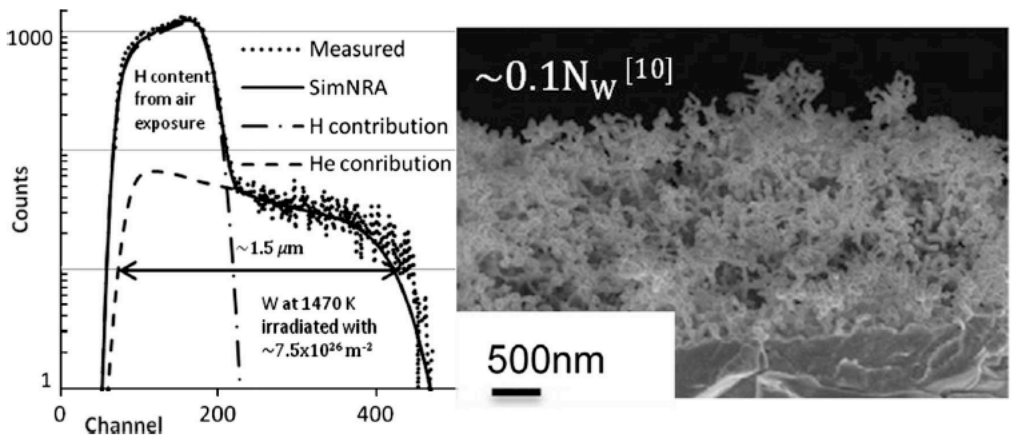

Fig. 23 (Right) Side view of tungsten nano-tendril "fuzz" produced in the high He flux-density Pilot-PSI linear plasma device. (Left) Post-exposure non-destructive Elastic Recoil Detection (ERD) provides depth profiles of the light elements. Hydrogen from air/water exposure and Helium from the plasma are shown and fit with a simulation. The higher channels correspond to closer to the surface [Woller_JNM13].

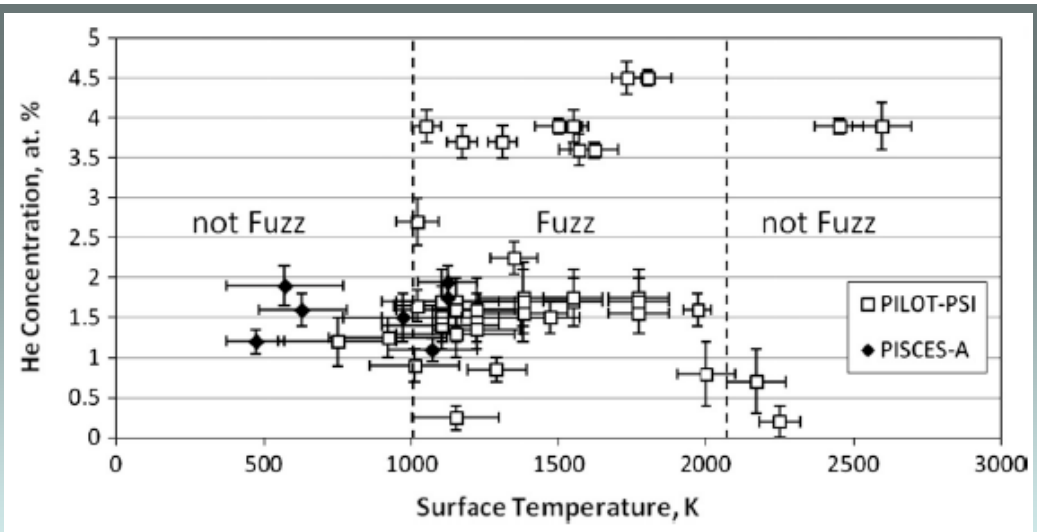

Fig. 24 ERD-measured average (W fuzz) and peak (non-W fuzz) He concentrations of samples from both PILOT-PSI (open square) and PISCES-A (solid diamond) of various surface temperatures exposed to various He fluences. W fuzz formation occurs in the temperature range between the dashed lines. Below this range, He is found in bubbles just in the surface. Above this range, pores are also present with the He bubbles. [Woller_JNM13]

Sample	T_s, *K*	Γ_{He}, 10^{20} $m^{-2}s^{-1}$	Φ_{He}, 10^{23} m^{-2}
a	1050	160	803
b	1043	100	629
High flux c	1107	100	415
d	1103	56	49
Low flux c	1087	2.5	--
e	1057	2.5	2.6
f	874	44	40
g	527	56	60

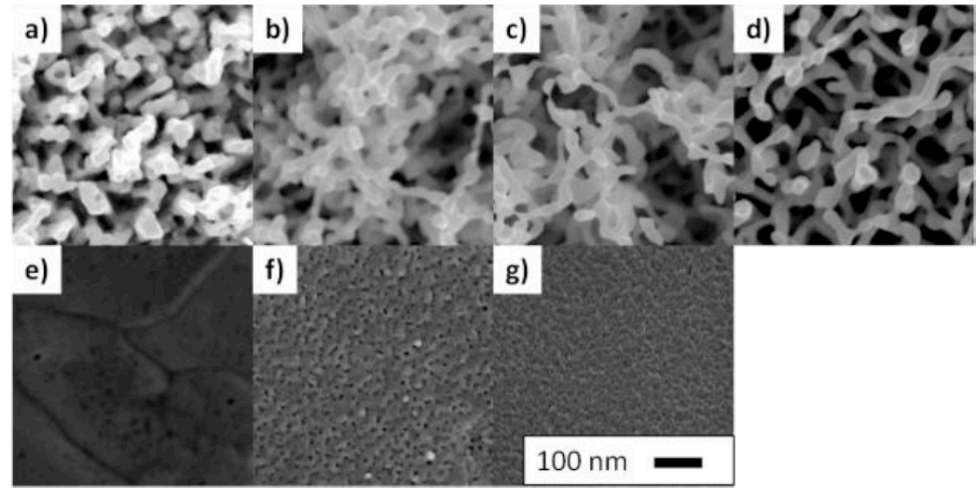

Fig. 25 (top) Summary of different He plasma exposures of tungsten samples in DIONISOS with accompanying real-time in situ Helium depth profiles (bottom) SEM micrographs of the tungsten surfaces. The appearing of nano-tendrils is evident in a)-d) while at low flux density and/or low sample temperature e)-g) the surface exhibits distortions consistent with bursted surface bubbles of helium, yet no nano-tendrils.

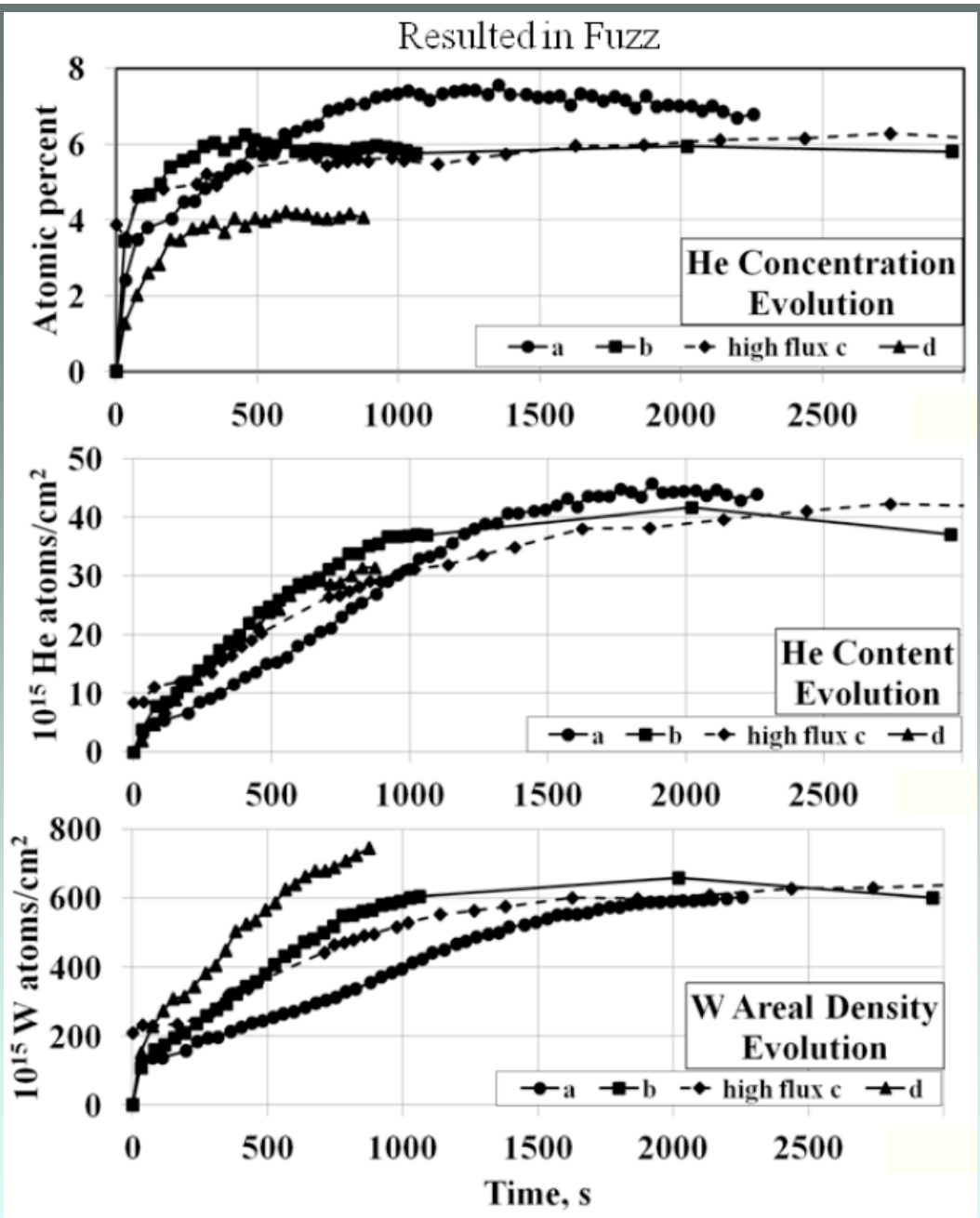

Fig. 26 Real-time, in situ measurements of tungsten nano-tendril evolution in DIONISOS for cases where tendrils grow (Fig. 25). (top) Average atomic concentration of Helium to W in tendril fuzz (middle) Absolute Helium areal density in tendrils (bottom)Absolute tungsten areal density (~depth) of tungsten in tendrils. [Woller_JNM14]

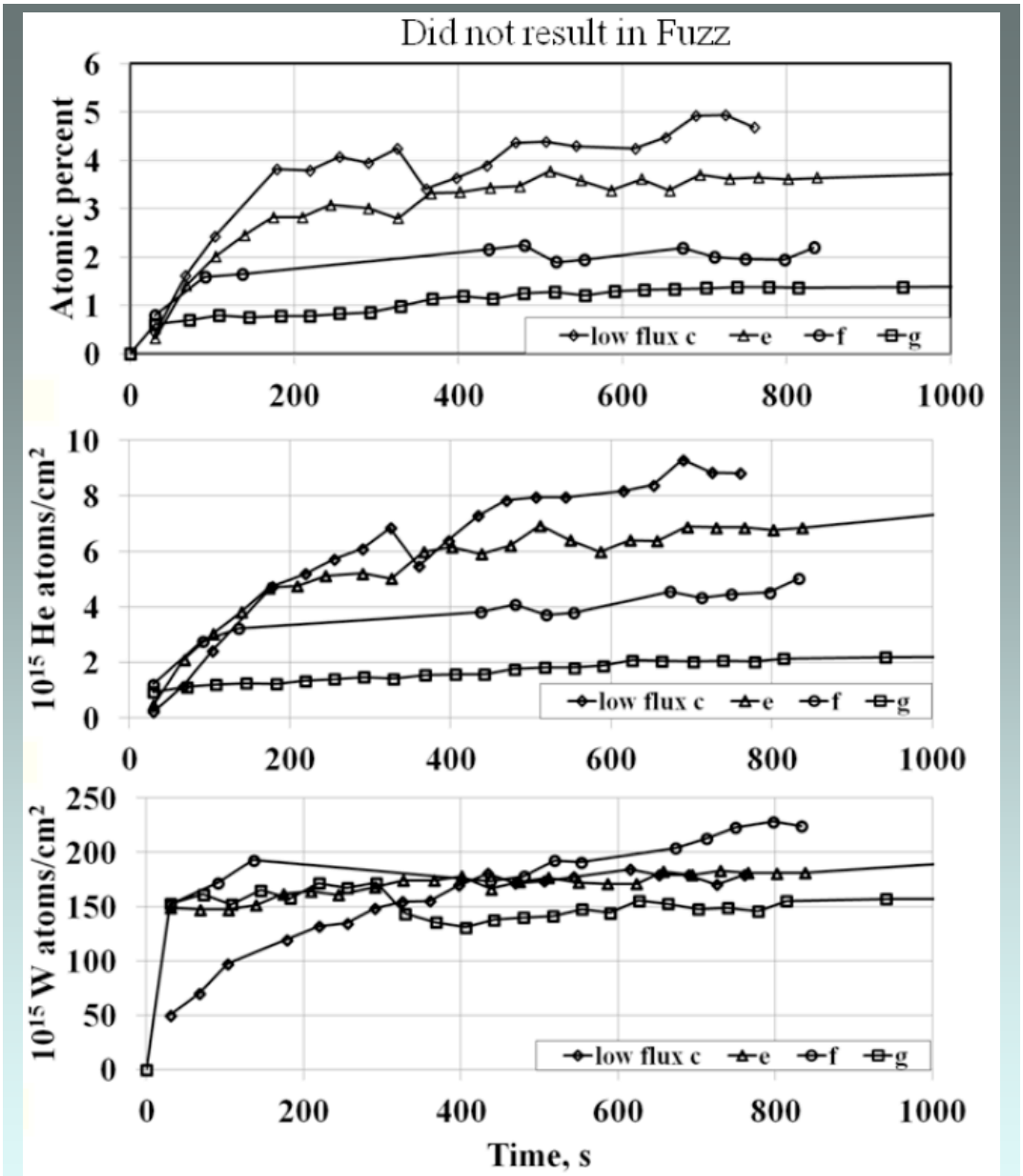

Fig. 27 Real-time, in situ measurements of tungsten nano-tendril evolution in DIONISOS for cases where He bubbles form but tendrils do not grow (Fig. 25). (top) Average atomic concentration of Helium to W in bubbles (middle) Absolute Helium areal density in bubbles (bottom) Absolute tungsten areal density (~depth) of tungsten involved in bubbles. [Woller_JNM14]

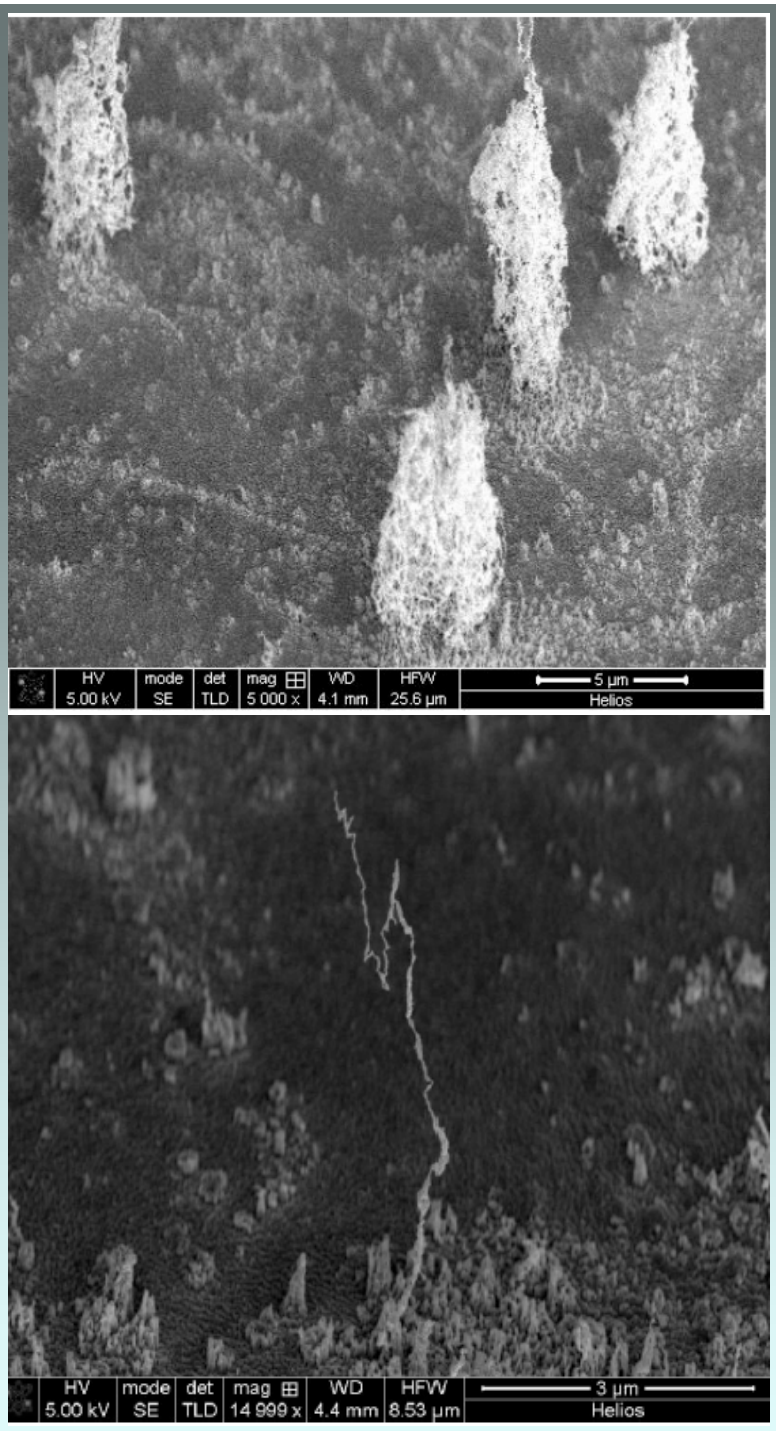

Fig. 28 SEM micrographs of tungsten nano-tendrils found on optically "shiny" parts of exposed samples in DIONISOS. (top) The tendrils form large (> 5 microns in height) isolated "haystacks" while the remainder of the surface has no tendrils (bottom) A tall (> 5 micron) isolated tendril haystack. In these regions the total amount of surface-average helium and tungsten tendrils is equal to that where uniform fuzz layers are found. [Woller_PhD15]

3.3. PSI Science On Confinement Devices

In recent years, there has been a push to better understand the interactions of He plasmas with PFCs materials such as refractory metals. He plasmas will be present in ITER and future fusion devices through aneutronic diagnostic plasma discharges and through the production of He ash from the D-T fusion reaction. One of the main thrusts of this research is in the understanding of the drastic change of surface morphology of refractory metal surfaces at elevated temperatures and under He plasma bombardment. This results in the formation of a dense interwoven layer of nano-tendrils on the surface of the refractory metal (Sec. 3.2). This layer of nano-tendrils, or "fuzz", can have significant effects, both beneficial and detrimental, on how the plasma interacts with the plasma-facing component. This surface morphology phenomenon was first observed and studied in linear plasma devices where surface, target and plasma conditions can all be controlled. Despite these severe morphology changes being very reproducible and consistent in a linear plasma device it was unclear whether or not the formation of these nano-tendrils would also be possible in the more dynamic, transient, and convoluted environment of a tokamak.

One of the key contributions and achievements of the PSI Science Center was to lead the study that demonstrated, for the first time, the growth of these nano-tendril structures in a tokamak [Wright_NF12]. This was achieved by leveraging the all-metal wall and high plasma heat-flux in Alcator C-Mod to find a set of plasma conditions to get the refractory metal PFC above the threshold temperature for nano-tendril growth ($T > 1000$ K), see Fig. 29 and Fig. 30. After repeated discharges to accumulate significant He ion fluence, the tiles of interest were removed and examined with SEM. SEM imaging clearly showed the formation of a significant nano-tendril layer on the tip of a tungsten Langmuir probe definitively showing that these fuzz layers can be grown in a tokamak (Fig. 31). The tungsten fuzz is built up and "survives" a very harsh environment, indeed one nearly identical to the ITER divertor: grazing angle magnetic field ~ 2-3 degrees, incident heat flux ~ 30 MW m^{-2} and parallel plasma heat flux >500 MW m^{-2}. This research was listed as a significant research result for the Alcator C-Mod program [Greenwald_NF13]. The growth of nano-tendrils in the C-Mod divertor was a prime example of the PSI Center's success at bridging across experiments and scales.

Further analysis of the W fuzz grown in Alcator C-Mod compared it to a W fuzz layer grown under similar conditions in the high-flux linear plasma device Pilot-PSI [Wright_JNM13]. Matching the surface morphology, layer thickness and surface temperatures showed that, within uncertainties, there is no significant difference between fuzz grown in tokamaks and linear plasma devices (see Fig. 32). This is an important connection to make as it suggests that the physics and mechanisms behind the nano-tendril growth are not affected by the tokamak environment. More practically, it allows understanding, predictions and projections based on experiments on linear plasma devices to be directly relatable and relevant for tokamaks as well. This result has had strong impact in the fusion community and motivated much more work with these

surfaces and consideration of possible impacts of these surfaces from a design and operations viewpoint for future devices, including ITER.

In addition to the direct studies on tungsten nano-tendrils on Alcator, the PSI Center contributed to the study of PMI on international fusion plasma devices due to its advanced surface diagnostic capabilities.

- The ERD measurements of Helium concentration in nano-tendrils has been studied on various linear plasma device (see Fig. 33 for an example) with contributions made to Pilot-PSI, Netherlands, [Temmerman_JNM14, Temmerman_JNM13], PISCES, USA (Fig. 33) and Japan [Ueda].

- The ion beam analysis tools of CLASS were used to trace impurity divertor transport on the DiMES probe [Chrobak_JNM14].

- The external beam of CLASS was used to trace tungsten migration through the Alcator C-Mod divertor due to erosion and transport processes [Barnard_JNM11]. This exercise demonstrated for the first time extremely low net erosion rates (<0.01 nm/s) for solid tungsten in a high flux density divertor.

- The CLASS facility was used to characterize tungsten redistribution in the Alcator C-Mod divertor region following large scale melting event [Lipschultz_NF12]. This is a topic of major concern for ITER and the PSI Center-Alcator collaboration revealed some of the first quantitative assessments of melt transport. Follow-up experiments have been carried out at JET for example.

The PSI Center research has also contributed more broadly to understanding the challenges of plasma-surface interactions in fusion reactors. This has included:

- Considering the effect of pressure limits at the separatrix in order to constrain the maximum allowed heat flux in the ITER divertor [Whyte_JNM13].

- A review article for the Materials Research Society on the overall challenges of fusion material modeling [Wirth_MRS11].

- A design study which carefully parametrized the necessary requirements of replicating the PMI figures of merit in scale down devices [Whyte_FED12]. This work was used to help design the VULCAN conceptual design for a compact (R~1 m) tokamak to study PMI at reactor conditions in true steady-state.

- A review article on the generic science and technology gaps and challenges for fusion materials [Zinkle_FED14]

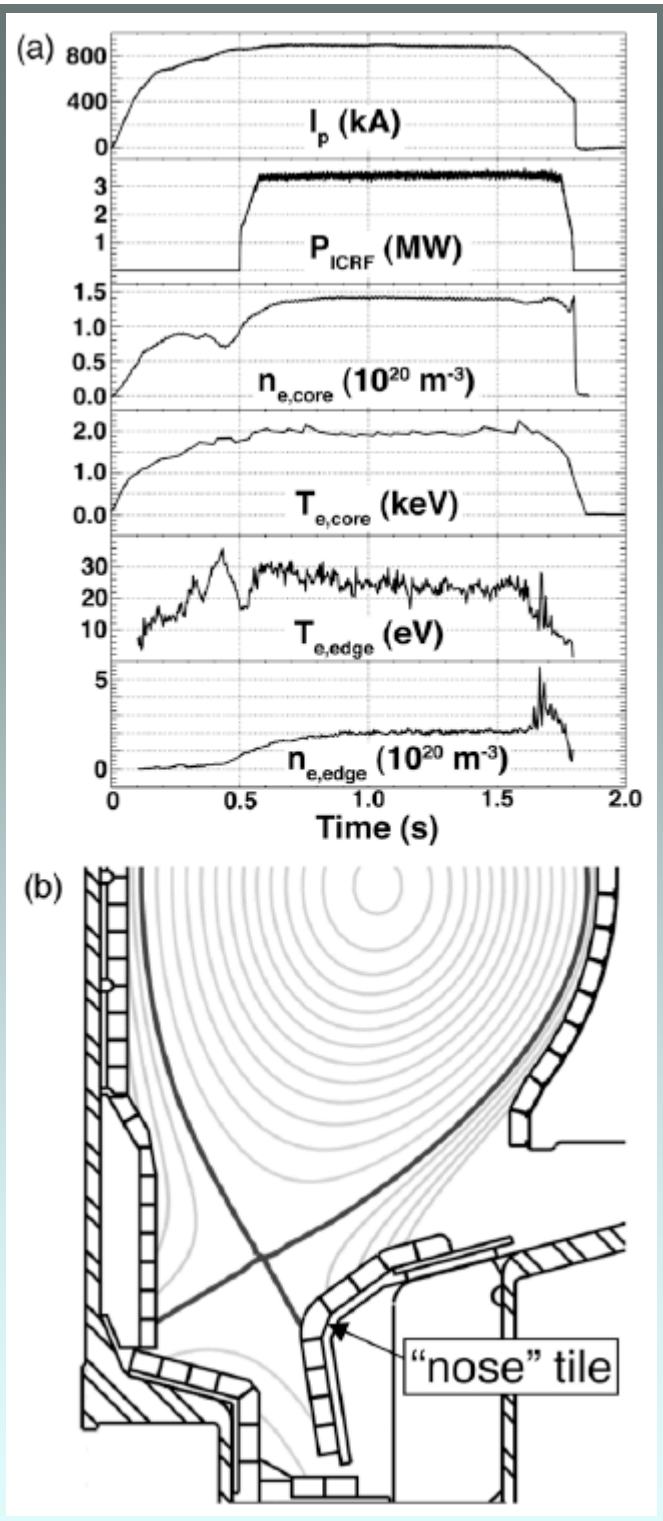

Fig. 29 PSI Center experiment for tungsten nano-tendril growth on Alcator C-Mod a) Time traces of plasma parameters for the 11 repeated He discharges designed to be conducive to nano-tendril growth b) Cross-section of C-Mod divertor and location of nose tile where tendrils grew. [Wright_NF12]

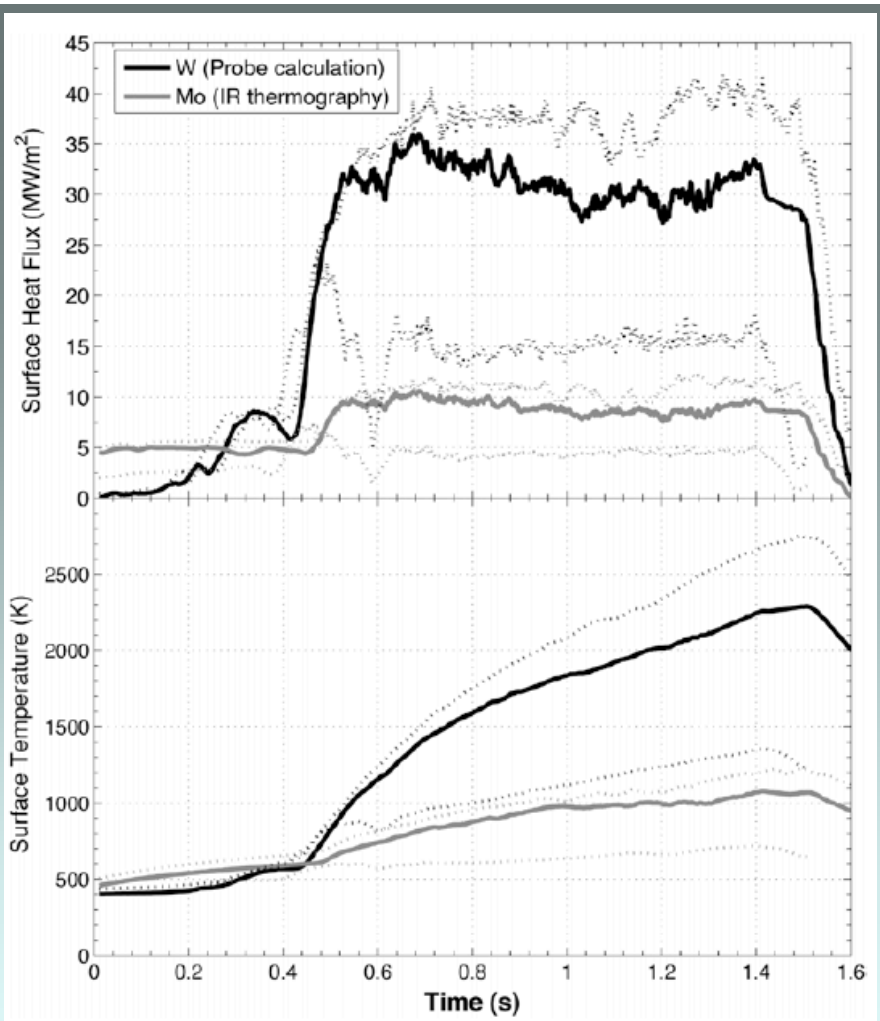

Fig. 30 (a) Surface heat flux and (b) surface temperature for the W probe and surrounding Mo surfaces during a plasma discharge. The solid lines represent the shot with the median heat flux/temperature for the 14-shot sequence. The dashed lines represent the shots with the maximum and minimum heat flux/temperature for the 14-shot sequence. [Wright_NF12]

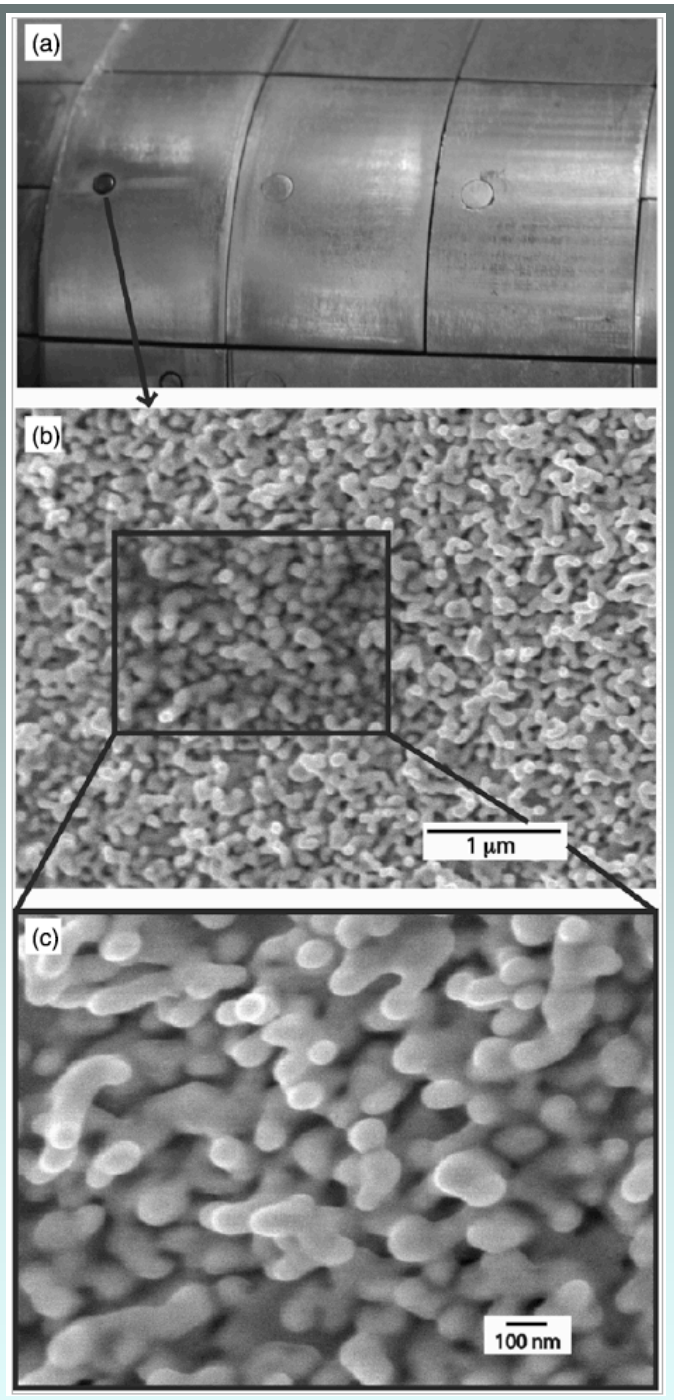

Fig. 31 (a) The ramped Mo tiles and W probe upon removal from Alcator C-Mod. The W probe, which is ramped in to the B field, is non-reflective compared to the other high-Z Mo surfaces(b) SEM image of the W probe surface showing nano-tendrils on the surface, and (c) high magnification SEM image showing the average thickness of the individual nano-tendrils to be ~100 nm thick. [Wright_NF12]

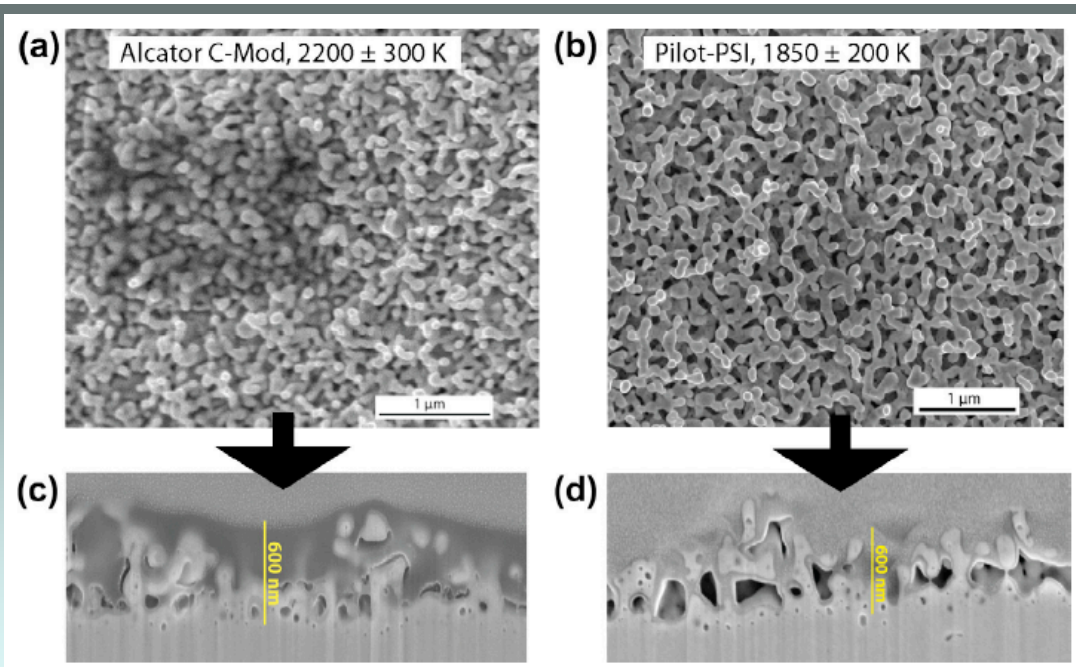

Fig. 32 (a) Surface nano-tendrils with characteristic thickness of 100 nm from the Alcator C-Mod W probe, (b) surface nano-tendrils with characteristic thickness of 100 nm from the linear Pilot-PSI W target, (c-d) cross-section of the W fuzz from C-Mod and Pilot-PSI respectively [Wright_JNM13]

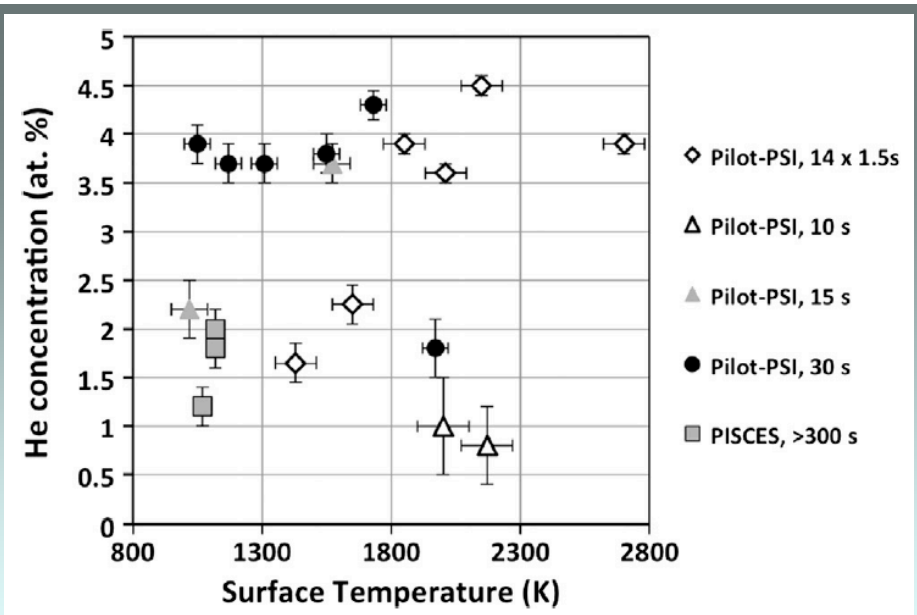

Fig. 33 Helium concentration in the surface morphology layer for various targets exposed in Pilot-PSI and PISCES-A as a function of surface temperature. Helium measurements from the CLASS facility [Wright_JNM13]

4. Outreach through Community Presentations

In the following section the presentations made by team members are documented. Where appropriate a comment (*in italics)* is made with respect to outreach to the broader science community. The presentations are organized by presenter and are oral presentations unless otherwise noted.

J. Safo

"Au^{3+} ion implantation depth markers to measure erosion and deposition in fusion relevant materials," poster, APS Division of Plasma Physics Annual Meeting, Denver CO (2013).

R. Sullivan

"Internal Physics of the Ion Sensitive Probe," poster, 20th Int. Conference on Plasma Surface Interactions in Controlled Fusion Devices, Aachen, Germany (2012).

"Plasma surface interactions in plasma thrusters," MIT Plasma Science and Fusion Seminar Series (2012)
Invited *Engaged fusion boundary scientists in commonalities to plasma thruster issues.*

"The development of Plasma-Surface Interaction diagnostic techniques," Rising Stars in Nuclear Science and Engineering (2013)
Invited *Conference featured prominent young female scientists in the broad area of nuclear science and engineering*

K. Woller

"Depth profiles of helium and deuterium in tungsten 'fuzz" using elastic recoil detection" poster, APS Division of Plasma Physics Annual Meeting, Chicago, IL (2010).

"Helium concentration in tungsten nano-tendril surface morphology using ERD," poster, 20th Int. Conference on Plasma Surface Interactions in Controlled Fusion Devices, Aachen, Germany (2012).

"Dynamic measurement of the helium concentration of evolving tungsten nanostructures using Elastic Recoil Detection during plasma exposure," poster, 21st Int. Conference on Plasma Surface Interactions in Controlled Fusion Devices, Japan (2014).

"Tungsten Fuzz: Analysis of plasma-material interactions using both in situ and post exposure surface science techniques" MIT NSE graduate student seminar (2014).

G. Wright

"Damage and analysis: The role of ion accelerators in plasma-surface interaction research," CAARI Conference on Application of Accelerators in Research & Industry, Fort Worth TX (2010).
Invited plenary talk *Multidisciplinary audience in research and industry*

"Tungsten migration in the Alcator C-Mod divertor," APS Division of Plasma Physics Annual Meeting, Chicago, IL (2010).

"Growth of tungsten nano-tendrils in the Alcator C-Mod Divertor," APS Division of Plasma Physics Annual Meeting, Salt Lake City, UT (2011)

"PFC activities and tungsten nano-tendril growth in Alcator C-Mod," US Plasma-Facing Components Workshop, Oak Ridge, TN, 2011

"Tungsten nano-tendril growth in the Alcator C-Mod divertor and the role of He," ITPA DIV-SOL Meeting, Aachen-Juelich, Germany, 2012
International expert group on fusion boundary plasmas

"Comparison of tungsten fuzz growth in Alcator C-Mod and linear plasma devices," International Conference on Plasma Surface Interactions in Controlled Fusion Devices, Aachen, Germany (2012)
Invited plenary talk

"Growth of tungsten nano-tendrils in the Alcator C-Mod divertor," APS Division of Plasma Physics Annual Meeting, Providence, RI (2012).
Invited talk *for general fusion scientist audience at DPP meeting*

"The role of the boundary plasma in defining the viability of magnetic fusion energy," Gaseous Electronic Conference, Princeton NJ (2013).
Plenary invited *for a general audience dealing with low temperature plasma physics.*

D. Whyte

"Taming the plasma-material interface as the next frontier," personal briefing to Associate Director for Office of Fusion Energy Science, Germantown, MD (2010)

"Taming the plasma-material interface as the next frontier," Princeton Plasma Physics Laboratory Colloquium, Princeton, NJ (2010)

"Plasma facing component challenges in magnetic fusion energy," 12th International Ceramics Congress & 5th Forum on New Materials, Montecatini Terme, Italy (2010)

"Implication of plasma-material interactions," Fusion Power Associates Annual Meeting, Washington DC (2010).

"Future of boundary plasma science," U. Wisconsin-Madison Plasma Colloquium, (2011)
"The extreme materials environment of fusion", MIT Industrial Liaison Program R&D Day (2011)
Invited *Wide-ranging audience of industrial R&D professionals interested in cutting-edge research in materials*

"Plasma-surface interaction challenges in fusion devices", Princeton Plasma Physics Lab Workshop on Magnetic Fusion Energy Roadmapping in ITER-era (2011).

"The future of boundary plasma and materials research for fusion," APS Sherwood Fusion Theory Annual Meeting, Atlanta, GA (2012)
Plenary Review *Fusion plasma theorists were engaged in understanding the complex multiscale physics associated with PSI science.*

"Tungsten and steels as plasma-facing components in DEMO", IAEA Workshop on Demonstration Fusion Reactors, Los Angeles (2012)
Plenary Review *PSI and material limitations for fusion DEMO designs*

"The role of the boundary plasma in defining the viability of magnetic fusion energy," APS Division of Plasma Physics Annual Meeting, Providence, RI (2012).
Plenary Review *for general fusion scientist audience at DPP meeting.*

"Advancing fusion energy materials research using ion beam analysis," International Conference on Ion Beam Analysis, Seatlle, WA (2013).
Plenary talk *Engagement with broader community using ion beam analysis of materials.*

"Exploring boundary plasma and plasma-material interaction research at MIT & Alcator C-Mod," U. Wisconsin-Madison, Plasma Physics Seminar, Madison WI (2014).

5. Grant Publications and Bibliography

In alphabetic order by first author

[Barnard_JNM11]

H. S. Barnard, B. Lipschultz and D. G. Whyte, "A study of tungsten migration in the Alcator C-Mod divertor," Journal of Nuclear Materials 415, S301-S304 (2011).

[Brunner_RSI13]

D. Brunner, B. LaBombard, R. Ochoukov, D, Whyte, "Scanning ion sensitive probe for plasma profile measurements in the boundary of the Alcator C-Mod tokamak," Review of Scientific Instruments 84 053507 (2013).

[Brunner_PPCF13]

D. Brunner, B. LaBombard, R. Ochoukov, R. Sullivan and D. Whyte, "Space-charge limits of ion sensitive probes," Plasma Physics and Controlled Fusion 55 (12) (2013).

[Chrobak_JNM14]

C. Chrobak, P.C. Stangeby, A.W. Leonard, D.L. Rudakov, C.P.C. Wong, A.G. McLean, G.M. Wright, D.A. Buchenauer, J.G. Watkins, W.R. Wampler, J.D. Elder, R.P. Doerner, D. Nishijima, G.R. Tynan," Measurements of gross erosion of Al in the DIII-D divertor," Journal of Nuclear Materials (2014).

[Greenwald_NF13]

M. Greenwald, A. Bader, S. Baek, H. Barnard, W. Beck, W. Bergerson, I. Bespamyatnov, M. Bitter, P. Bonoli, M. Brookman, D. Brower, D. Brunner, W. Burke, J. Candy, M. Chilenski, M. Chung, M. Churchill, I. Cziegler, E. Davis, G. Dekow, L. Delgado-Aparicio, A. Diallo, W. Ding, A. Dominguez, R. Ellis, P. Ennever, D. Ernst, I. Faust, C. Fiore, E. Fitzgerald, T. Fredian, O.E. Garcia, C. Gao, M. Garrett, T. Golfinopoulos, R. Granetz, R. Groebner, S. Harrison, R. Harvey, Z. Hartwig, K. Hill, J. Hillairet, N. Howard, A.E. Hubbard, J.W. Hughes, I. Hutchinson, J. Irby, A.N. James, A. Kanojia, C. Kasten, J. Kesner, C. Kessel, R. Kube, B. LaBombard, C. Lau, J. Lee, K. Liao, Y. Lin, B. Lipschultz, Y. Ma, E. Marmar, P. McGibbon, O. Meneghini, D. Mikkelsen, D. Miller, R. Mumgaard, R. Murray, R. Ochoukov, G. Olynyk, D. Pace, S. Park, R. Parker, Y. Podpaly, M. Porkolab, M. Preynas, I. Pusztai, M. Reinke, J. Rice, W. Rowan, S. Scott, S. Shiraiwa, J. Sierchio, P. Snyder, B. Sorbom, V. Soukhanovskii, J. Stillerman, L. Sugiyama, C. Sung, D. Terry, J. Terry, C. Theiler, N. Tsujii, R. Vieira, J. Walk, G. Wallace, A. White, D. Whyte, J. Wilson, S. Wolfe, K. Woller, G. Wright, J. Wright, S. Wukitch, G. Wurden, P. Xu, C. Yang and S. Zweben, "Overview of

experimental results and code validation activities at Alcator C-Mod," Nuclear Fusion 53 104004 (2013).

[Lipschultz_NF12]

B. Lipschultz, J.W. Coenen, H.S. Barnard, N.T. Howard, M.L. Reinke, D.G. Whyte, G.M. Wright, "Divertor tungsten tile melting and its effect on core plasma performance," Nuclear Fusion 52 123002 (2012).

[Peterson_SB13]

E. Peterson, "Real-time Rutherford backscattering spectroscopy analysis of plasma erosion in DIONISOS," MIT Nuclear Science and Engineering, S.B. Thesis (2013) *http://hdl.handle.net/1721.1/82448.*

[Safo_MS14]

J.K. Safo, "Stability of gold depth markers in plasma facing component high-Z refractory metals relevant for nuclear fusion," MIT Nuclear Science and Engineering, M.S. Thesis (2014).

[Sullivan_JNM13]

R.M. Sullivan, R. Ochoukov, D.G. Whyte, "Internal physics of the ion-sensitive probe," Journal of Nuclear Materials, 438S, 1253-1256 (2013).

[Sullivan_NIMB14]

R. M. Sullivan, A. Pang, M. Martinez-Sanchez and D. G. Whyte, "A lithium depth-marker technique for rapid erosion and deposition measurements," Nuclear Instruments & Methods in Physics Research Section B-Beam Interactions with Materials and Atoms 319, 79-86 (2014).

[Sullivan_NIMB15]

R.M. Sullivan, J.K. Safo, D.G. Whyte, "Suitability of a Li depth marker-based erosion measurement in boron nitride at elevated temperatures," in review at Nuclear Instruments and Methods B (2014)

[Temmerman_JNM13]

G. De Temmerman, K. Bystrov, R.P. Doerner, L. Marot, G.M. Wright, K.B. Woller, D.G. Whyte, J.J. Zielinski "Helium effects on tungsten under fusion-relevant plasma loading conditions," Journal of Nuclear Materials, 438S, 78-83, July 2013.

[Temmerman_JNM14]

G. De Temmerman, T.W. Morgan, G.G. van Eden, T. de Kruif, M. Wirtz, J. Matejicek, T. Chraska, R.A. Pitts, G.M. Wright, "Effect of high-flux H/He plasma exposure on tungsten damage due to transient heat loads," Journal of Nuclear Materials, *in Press*, doi:10.1016/j.jnucmat.2014.09.075

[Ueda_JNM13]

Y. Ueda, H.Y. Peng, H.T. Lee, N. Ohno, S. Kajita, N. Yoshia, R. Doerner, G. De Temmerman, V. Alimov, G. Wright, "Helium effects on tungsten surface morphology and deuterium retention," Journal of Nuclear Material, 442 S267 (2013).

[Whyte_FED12]

D.G. Whyte, G.M. Olynyk, H.S. Barnard, P.T. Bonoli, L. Bromberg, M.L. Garrett, C.B. Haakonsen, Z.S. Hartwig, R.T. Mumgaard, Y.A. Podpaly, "Reactor similarity for plasma-material interactions in scaled-down tokamaks as the basis for the Vulcan conceptual design," Fusion Engineering and Design 87 (2012).

[Whyte_JNM13]

D. G Whyte, B. LaBombard, J.W. Hughes, B. Lipschultz, J. Terry, D. Brunner, P.C. Stangeby, D. Elder, A.W. Leonard, J. Watkins "Constraining the divertor heat width in ITER, " Journal of Nuclear Materials, 438S, 435-439 (2013).

[Wirth_MRS11]

B. D. Wirth, K. Nordlund, D. G. Whyte and D. Xu, "Fusion materials modeling: Challenges and opportunities," Material Research Society Bulletin 36 (3), 216-222 (2011).

[Woller_JNM13]

K.B. Woller, D.G. Whyte, G.M. Wright, R.P. Doerner, G. de Temmerman, "Helium concentration in tungsten nano-tendril surface morphology using Elastic Recoil Detection," Journal of Nuclear Materials, 438S, 913-916 (2013).

[Woller_JNM14]

K.B. Woller, D.G. Whyte, G.M. Wright, "Dynamic measurement of the helium concentration of evolving tungsten nanostructures using Elastic Recoil Detection during plasma exposure," in press Journal of Nuclear Materials (2014)

[Woller_PhD15]

K.B. Woller, "Tungsten fuzz: Analysis of plasma-material interactions using both in situ and post exposure surface science techniques," MIT Nuclear Science and Engineering, Ph.D Thesis *in progress* (2015).

[Wright_AIP11]

G.M. Wright, H.S. Barnard, Z.S. Hartwig, P.W. Stahle, R.M. Sullivan, K.B. Woller, D.G. Whyte, "Plasma-surface interaction research at the Cambridge Laboratory of Accelerator Studies of Surfaces," AIP Conference Proceedings, 1336, 626 (2011).

[Wright_NF12]

G.M. Wright, D. Brunner, M.J. Baldwin, R.P. Doerner, B. Labombard, B. Lipschultz, J.L. Terry, D.G. Whyte, "Tungsten nano-tendril growth in the Alcator C-Mod divertor," Nuclear Fusion 52 (2012).

[Wright_JNM13]

G. M. Wright, D. Brunner, D. Baldwin, M.J. Bystrov, R.P. Doerner, B. LaBombard, B. Lipschultz, G. De Temmerman, J.L. Terry, D.G. Whyte, K.B. Woller, "Comparison of tungsten nano-tendrils grown in Alcator C-Mod and linear plasma devices," Journal of Nuclear Materials, 438S, 84-89 (2013).

[Wright_RSI14]

G. M. Wright, H. A. Barnard, L. A. Kesler, E. E. Peterson, P. W. Stahle, R. M. Sullivan, D. G. Whyte and K. B. Woller, "An experiment on the dynamics of ion implantation and sputtering of surfaces," Review of Scientific Instruments 85 023503 (2014).

[Wright_JNM14a]

G.M. Wright, G.G. van Eden, L.A. Kesler, G. De Temmerman, D.G. Whyte, K.B. Woller, "Characterizing the recovery of a solid surface after tungsten nano-tendril formation," Journal of Nuclear Materials, *in Press*, doi:10.1016/j.jnucmat.2014.11.083

[Wright_JNM14b]

G.M. Wright, M.G. Durrett, K.W. Hoover, L.A. Kelser, D.G. Whyte, "Silicon Carbide as a tritium permeation barrier in tungsten plasma-facing components," Journal of Nuclear Materials, *submitted and corrected, awaiting final approval*.

[Zinkle_FED14]

S. J. Zinkle, J. P. Blanchard, R. W. Callis, C. E. Kessel, R. J. Kurtz, P. J. Lee, K. A. McCarthy, N. B. Morley, F. Najmabadi, R. E. Nygren, G. R. Tynan, D. G. Whyte, R. S. Willms and B. D. Wirth, "Fusion materials science and technology research opportunities now and during the ITER era," Fusion Engineering and Design 89 (7–8), 1579-1585 (2014).